HHS Public Access

Author manuscript

Neuroscience. Author manuscript; available in PMC 2019 March 15.

Published in final edited form as:

Neuroscience. 2018 March 15; 374: 155–171. doi:10.1016/j.neuroscience.2018.01.046.

Human *TUBB3* Mutations Disrupt Netrin Attractive Signaling

Huai Huang[†], **Tao Yang**[†], **Qiangqiang Shao**, **Tanushree Majumder**, **Kristopher Mell**, and **Guofa Liu**

Department of Biological Sciences, University of Toledo, 2801 West Bancroft St., Toledo, OH 43606, USA

Abstract

Heterozygous missense mutations in human *TUBB3* gene result in a spectrum of brain malformations associated with defects in axon guidance, neuronal migration and differentiation. However, the molecular mechanisms underlying mutation-related axon guidance abnormalities are unclear. Recent studies have shown that netrin-1, a canonical guidance cue, induced the interaction of TUBB3 with the netrin receptor deleted in colorectal cancer (DCC). Furthermore, TUBB3 is required for netrin-1-induced axon outgrowth, branching and pathfinding. Here, we provide evidence that *TUBB3* mutations impair netrin/DCC signaling in the developing nervous system. The interaction of DCC with most TUBB3 mutants (eight out of twelve) is significantly reduced compared to the wild type TUBB3. TUBB3 mutants R262C and A302V exhibit decreased subcellular colocalization with DCC in the growth cones of primary neurons. Netrin-1 increases the interaction of endogenous DCC with wild type human TUBB3, but not R262C or A302V, in primary neurons. Netrin-1 also increases co-sedimentation of DCC with polymerized microtubules (MTs) in primary neurons expressing the wild type TUBB3, but not R262C or A302V. Expression of either R262C or A302V not only suppresses netrin-1-induced neurite outgrowth, branching and attraction *in vitro*, but also causes defects in spinal cord commissural axon (CA) projection and pathfinding *in ovo*. Our study reveals that missense *TUBB3* mutations specifically disrupt netrin/DCC-mediated attractive signaling.

Keywords

Netrin-1; DCC; TUBB3; Missense Mutations; Signal Transduction; Axon Guidance; Commissural Axons

[‡]To whom correspondence should be addressed: Guofa Liu, Department of Biological Sciences, University of Toledo, 2801 West Bancroft St., Toledo, OH 43606, USA, Tel: (419) 530-2869; Fax: (419) 530-7737; Guofa.Liu@utoledo.edu.
[†]H. H. and T. Y. contributed equally to this work.

Conflict of interest

The authors declare no conflicts of interest.

1. Introduction

During brain development, temporospatial modulation of microtubule (MT) dynamics in the growth cone (GC) of developing post-mitotic neurons plays an essential and instructive role for axon projection and pathfinding (Buck and Zheng, 2002; Challacombe et al., 1997; Dent et al., 2004; Dent et al., 2011; Kalil and Dent, 2005; Lee and Suter, 2008; Lei et al., 2012; Liu and Dwyer, 2014; Purro et al., 2008; Sabry et al., 1991; Suh et al., 2004; Tanaka et al., 1995). Mutations in α- and β-tubulin-encoding genes (e.g. *TUBA1A, TUBB2A, TUBB4A, TUBB2B, TUBB3* and *TUBA8*) cause a variety of brain malformations (Abdollahi et al., 2009; Cushion et al., 2013; Guerrini et al., 2012; Jaglin et al., 2009; Kumar et al., 2010; Liu and Dwyer, 2014; Poirier et al., 2010; Tischfield et al., 2010; Tischfield et al., 2011), such as lissencephaly, polymicrogyria, hypoplasia of the internal capsule, basal ganglia, the hippocampus, cerebellum, brainstem, and cranial nerves, and partial or complete agenesis of the commissural fiber tracts and the corticospinal tract. The disease-associated *TUBB3* mutations have recently been shown to impair tubulin heterodimer formation and alter MT instability, resulting in a spectrum of axonal guidance defects including agenesis or hypoplasia of commissural axon (CA) tracts, the corticospinal tract, the anterior commissure and oculomotor nerves (Poirier et al., 2010; Tischfield et al., 2010). TUBB3$^{R262C/R262C}$ knock-in disease mouse model further reveals specific axon guidance defects in CAs and cranial nerves: partial or complete absence of the corpus callosum and the anterior commissure as well as misguidance of multiple cranial nerves (Poirier et al., 2010; Tischfield et al., 2010). However, it is unclear why *TUBB3* mutations are associated with these axon projection defects, such as those involved in CA guidance, when TUBB3, a neuron-specific beta III tubulin, is widely expressed in all developing neurons.

Netrins, a family of canonical guidance cues, are known to play an essential role in axon guidance and neuronal migration (Alcantara et al., 2000; Colamarino and Tessier-Lavigne, 1995; Hedgecock et al., 1990; Ishii et al., 1992; Kennedy et al., 1994; Kolodziej et al., 1996; Tessier-Lavigne et al., 1988). The mammalian receptors of netrins are deleted in colorectal cancer (DCC) (Fazeli et al., 1997; Keino-Masu et al., 1996), neogenin (Keeling et al., 1997; Keino-Masu et al., 1996), uncoordinated-5 (UNC5) (Ackerman et al., 1997; Leonardo et al., 1997), and Down syndrome cell adhesion molecule (DSCAM) (Liu et al., 2009; Ly et al., 2008). Netrin-1- and DCC-deficient mice exhibit similar phenotypic defects in axon guidance and neuronal migration, including a reduction in the number of CAs, shortening and misrouting of axons in the spinal cord, lack of the corpus callosum and hippocampal commissure, reduction in the size of the anterior commissure, absence of the pontine nuclei in the brain, and optic nerve hypoplasia (Burgess et al., 2006; Deiner et al., 1997; Fazeli et al., 1997; Serafini et al., 1996). Our recent studies indicate that netrin-1 can directly regulate MT dynamics through the interaction of its receptor DCC to TUBB3 during axon attraction (Qu et al., 2013a). Knockdown of TUBB3 not only blocks netrin-1 induced axon outgrowth, branching and attraction *in vitro*, but also inhibits spinal cord CA projection and pathfinding *in vivo*, suggesting that TUBB3 is specifically involved in netrin-1/DCC-mediated axon projection (Huang et al., 2015; Qu et al., 2013a).

In the present study, we examined the functional importance of *TUBB3* mutations in netrin/DCC signaling through *in vitro* and *in vivo* approaches. Our results indicate that

TUBB3 mutations may disrupt the coupling of netrin/DCC signaling with MT dynamics, resulting in specific defects of netrin-mediated axon projection and pathfinding in the developing nervous system.

2. Experimental Procedures

2.1. Materials

Plasmids encoding the full-length human TUBB3, DCC and TUBB3 mutants (G82R, T178M, E205K, M388V and A302V, gifts from Dr. Jamel Chelly) have been described previously (Huang et al., 2015; Li et al., 2004a; Poirier et al., 2010; Qu et al., 2013a; Shao et al., 2017). Using wild type human TUBB3 as a template, site-directed mutagenesis was performed to generate human missense TUBB3 mutants and verified by sequencing. The following oligonucleotide primers were used in the PCR reactions: 5’ forward primer 5’-GTGCCCTTCCCGCAACTGCACTTCTTC-3’ and 3’ reverse primer 3’-GAAGAAG TGCAGTTGCGGGAAGGGCAC-5’ for R62Q; 5’ forward primer 5’-GTGCCCTTCCCGTGCCTGCA CTTCTTC-3’ and 3’ reverse primer 3’-GAAGAAGTGCAGGCACGGGAAGGGCAC-5’ for R262C; 5’ forward primer 5’-AACATGATGGCCACCTGCGACCCGCGC-3’ and 3’ reverse primer 3’-GCGCG GGTCGCAGGTGGCCATCATGTT-5’ for A302T; 5’ forward primer 5’-GGCCGCATGTCCGTTAA GGAGGTGGAC-3’ and 3’ reverse primer 3’-GTCCACCTCCTTAACGGACATGCGGCC-5’ for M323V; 5’ forward primer 5’-ATGGAGTTCACCAAAGCCGAGAGCAAC-3’ and 3’ reverse primer 3’-GTTGCTCTCGGCTTTGGTGAACTCCAT-5’ for E410K; 5’ forward primer 5’-AGCAACATGAACC ACCTGGTGTCCGAG-3’ and 3’ reverse primer 3’-CTCGGACACCAGGTGGTTCATGTTGCT-5’ for D417H; and 5’ forward primer 5’-AGCAACATGAACAACCTGGTGTCCGAG-3’ and 3’ reverse primer 3’-CTCGGACACCAGGTTGTTCATGTTGCT-5’ for D417N. FLAG-tagged TUBB3 truncations TUBB3-1-232 and TUBB3-233-449 were constructed between the EcoR I and Xba I sites in the pcDNA3.1 (−) vector. The following primers are used for the PCR reactions: 5’ forward primer 5’-CCG GAATTCATGAGGGAGATCGTGCACATC-3’ and 3’ reverse primer 3’-GCTCTAGATCACTTGTCG TCATCGTCTTTGTAGTCGGTGGCCGATACCAGGTG-5’ for TUBB3-1-232; 5’ forward primer 5’-CCGGAATTCATGAGCGGAGTCACCACCTC-3’ and 3’ reverse primer 3’-GCTCTAGATCACTTG TCGTCATCGTCTTTGTAGTCCTTGGGGCCCTGGGC-3’ for TUBB3-233-449. TUBB3 shRNAs were designed to target the 3' untranslated region (UTR) of human and mouse TUBB3. The targeted sequences of control shRNA and TUBB3 shRNA #3 and #4 are: 5’-CCCCCACTCCATGTGAGTT-3’ (control shRNA), 5’-AGGTTAAAGTCCTTCAGTG-3’ (#1) and 5’-GCAGCCAGGGCCAAGACAG-3’ (#4), respectively. The oligonucleotide templates were inserted into the mU6pro vector between the Xba I and the EcoR I sites and verified by sequencing.

The following antibodies were used: rabbit anti-FLAG, and rabbit anti-TUBB3 (Abcam, Cambridge, MA, USA); mouse anti-DCC (BD Biosciences, San Jose, CA, USA); mouse anti-TUBB3 (Covance, Princeton, New Jersey, USA); mouse anti-Myc (Calbiochem, Rockland, MA, USA); Alexa Fluor® 488 goat anti-mouse IgG and Alexa Fluor® 647 goat

anti-rabbit IgG (Invitrogen, Grand Island, NY, USA); the HRP-conjugated anti-rabbit and anti-mouse secondary antibodies (Santa Cruz Biotechnology, Lexington, NY). Purified chick netrin-1 protein was either purchased from R&D (Minneapolis, MN, US) or purified with anti-Myc tag affinity matrix from conditioned media of HEK cells stably expressing netrin-1 (Liu et al., 2004; Liu et al., 2007; Liu et al., 2009). The sham-purified control solution was made from the conditioned media of HEK cells which do not express netrin-1. Paclitaxel (taxol) was obtained from Cayman Chemical (Ann Arbor, MI, USA). Alexa Fluor 555 phalloidin and DAPI were purchased from Invitrogen (Carlsbad, California).

2.2. Co-immunoprecipitation (co-IP) and Western analysis

HeLa cells were transfected with the PEI method. Primary E15 cortical neurons were nucleofected and cultured in DMEM supplemented with 10% fetal bovine serum (FBS) and 10 U/ml penicillin/streptomycin overnight. For netrin-1 stimulation, primary neurons were further cultured in FBS-free DMEM media supplemented with B27 for 6 h, and then treated with either purified netrin-1 protein (250 ng/ml) or sham purified control up to 20 min. For Co-IP, primary neurons and HeLa cells were lysed using MLB cell lysis buffer (50mM Tris-HCl, 100mM NaCl, 1% NP-40, and 0.1% PMSF) mixed with Roche protease inhibitor cocktail tablets (cOmplete tablets, Mannheim, Germany) for 20 min on ice. Supernatant was collected after centrifugation (at 10,000 × g, 20 min) and incubated with specific antibodies and protein A/G-agarose beads (Santa Cruz Biotechnology) overnight at 4 °C. Protein extracts were separated with 7.5% SDS-polyacrylamide gel electrophoresis (PAGE) and immunoblotted with specific primary antibodies. After incubation with specific secondary antibodies, western blots were visualized with the enhanced chemiluminescence kit (Fisher, Pittsburgh, PA).

2.3. MT cosedimentation assay

Primary cortical neurons from E15 mouse cortexes were dissociated, nucleofected and stimulated with purified netrin-1 (250 ng/ml) or sham-purified control for 20 min as previously described (Huang et al., 2015; Qu et al., 2013a). Primary neurons were lysed in the MLB buffer mixed with protease inhibitor cocktail tablets. Cell lysates were centrifuged at 10,000 × g for 20 min at 4°C and the supernatant was then incubated with 40 μM taxol or DMSO in PEMG buffer (100 mM PIPES, 1 mM EGTA, 1 mM MgSO4, 1 mM GTP, pH 6.8) at room temperature for 30 min. In a 10% sucrose cushion solution, MTs were pelleted after centrifugation at 50,000 × g for 30 min at 20°C as previously described (Huang et al., 2015; Qu et al., 2013a; Shao et al., 2017). Both supernatant and pellet fractions were collected, and the pellet was then resuspended in tubulin buffer (50 mM HEPES, 1 mM $MgCl_2$, 1mM EGTA, 10% glycerol, 150 mM KCl, 40 μM taxol, 1 mM GTP, 5 mM Mg-ATP, 1 mM PMSF, 1× protease inhibitor mixture). Proteins in the supernatant and the pellet were separated by 7.5% SDS-PAGE and detected by Western blotting.

2.4. Immunofluorescence and colocalization analysis

After nucleofection, primary E15 cortical neurons were grown on PLL-coated coverslips overnight, fixed in pre-warmed 4% paraformaldehyde (PFA) in DMEM and permeabilized with 0.3% Triton X-100 in PBS at room temperature for 30 min. Cells were then blocked with 3% BSA in PBS containing 0.1% Triton X-100 at room temperature for 1h and

incubated with mouse anti-DCC (1:1000) and rabbit anti-FLAG (1:5000) primary antibodies overnight at 4°C. Neurons were incubated with fluorescent secondary antibodies (Alexa Fluor donkey anti-mouse IgG and Alexa Fluor 647 donkey anti-rabbit IgG) for 2 h at 37 °C and coverslips with neurons were mounted onto glass slides with Fluorogel (Electron Microscopy Sciences). Fluorescent images of axonal growth cones were taken sequentially using Leica SP8 confocal microscope with a HyD detector in photon counting mode. The Pearson Correlation Coefficient (PCC) in each region of interest (ROI) of the GC was obtained using the Leica confocal software and PCC values were analyzed using GraphPad Software.

2.5. Primary neuron cultures and analysis of neurite outgrowth and axon branching

The procedures of primary neuron dissociation, culture and nucleofection were conducted as described previously with some modifications (Huang et al., 2015). E15 cortical neurons were dissociated and nucleofected with Venus YFP plus missense human TUBB3 mutants, TUBB3 control shRNA, TUBB3 shRNAs (combination of TUBB3 shRNA #1 and #4), TUBB3 shRNAs plus wild type human TUBB3 or TUBB3 shRNAs plus TUBB3 mutants (Amaxa Biosystems). After nucleofection, cortical neurons were left settling on the PLL coated-coverslips for 3 h in the culture medium (DMEM +10% FBS + Penicillin/streptomycin) and the culture medium was replaced by fresh DMEM with B27 (Invitrogen). For examining neurite outgrowth, primary neurons were cultured at 37°C with 5% CO2 for 20 h in the presence of either purified netrin-1 (250 ng/ml) or the sham-purified control. Neurons were then fixed with 4% pre-warmed PFA dissolved in the DMEM medium for 30 min at 37°C and stained with the Alexa Fluor® 555 phalloidin (Molecular Probes, NY, USA) and a DNA-specific probe DAPI (Invitrogen, CA, US). Images were taken using Leica TCS SP8 confocal microscope and the longest neurite (axon) length was examined using NIH ImageJ program.

For examining axon branching, primary neurons were cultured on PLL-coated coverslips for 72 h after nucleofection in the presence of purified chick netrin-1 (250 ng/ml) or sham-purified control as previously described (Huang et al., 2015). Cells were then fixed with pre-warmed 4% PFA for 30 min at 37 °C, permeabilized with 0.3% Triton X-100, and blocked with 3% BSA in PBS plus 0.1% Triton at room temperature. Neurons were stained with DAPI and BODIPY® 558/568 Phalloidin (1;100 in PBS) for 2 h at 37 °C. Fluorescent images were taken with a confocal microscope (Leica, TCS SP8) and an axon branching point at a clearly polarized axon with a branch longer than 10 μm was calculated using NIH ImageJ program.

2.6. Chick Spinal Cord CA Turning Assay

Fertilized White Leghorn chick embryos were incubated and staged as described previously (Hamburger et al., 1992; Li et al., 2008; Liu et al., 2004; Liu et al., 2007; Liu et al., 2009; Qu et al., 2013a; Qu et al., 2013b). At stage 12–15, either Venus YFP only or combination of Venus YFP with specific plasmids were introduced into the neural tube and the *in ovo* electroporation was performed (Li et al., 2008; Liu et al., 2004; Liu et al., 2007; Liu et al., 2009; Qu et al., 2013a; Qu et al., 2013b; Shao et al., 2017). YFP-labeled spinal cords at stage 18–20 were collected and trimmed into rectangular explants. The spinal cord explants

with the floor plate were co-cultured with an aggregate of control or netrin-1 secreting HEK cells as described previously (Li et al., 2008; Liu et al., 2004; Liu et al., 2007; Liu et al., 2009; Qu et al., 2013a; Qu et al., 2013b; Shao et al., 2017). After fixation with 4% PFA, the samples were mounted in Gel/Mount and images were taken under the Leica SP8 confocal microscope. Axons turning towards the HEK cell aggregate more than 5° were defined as turning axons and the percentage of attracting axons was analyzed using NIH ImageJ program.

2.7. Chick Spinal Cord CA Projection *in Vivo*

The chick *in ovo* neural tube electroporation at stage 12–15 was performed and YFP-labelled spinal cords between stages 22–23 after electroporation were isolated as previously described (Fitzli et al., 2000; Li et al., 2008; Liu et al., 2007; Liu et al., 2009; Qu et al., 2013a; Qu et al., 2013b; Shao et al., 2017; Stoeckli et al., 1997). The lumbosacral region of the spinal cord with YFP fluorescence was collected, fixed with 4% PFA, and sectioned transversely at a thickness of 200 μm. The spinal cord slices were transferred on slides and mounted in Fluorogel. Images were taken under the Leica SP8 confocal microscope. The number of fluorescent axons reaching or crossing over the midline, the total numbers of axons and the axon distance from the midline were calculated as previously described (Li et al., 2008; Liu et al., 2007; Liu et al., 2009; Qu et al., 2013a; Qu et al., 2013b; Shao et al., 2017). The percentage of axons reaching the spinal cord midline, average axonal distance from the midline and percentage of embryos with misguided axons were analyzed using the Leica confocal software (LAS AF Lite).

3. Results

3.1. *TUBB3* mutations impair the interaction of DCC with TUBB3

Our recent studies have shown that the direct interaction of DCC with TUBB3 is required for netrin/DCC signaling (Qu et al., 2013a). To determine whether missense *TUBB3* mutations affect the interaction with DCC, plasmids expressing full-length human DCC (DCC-Myc) were co-transfected with either full-length human TUBB3 tagged with FLAG (TUBB3-FLAG) or FLAG-tagged TUBB3 mutants (G82R, T178M, E205K, A302V, A302T, M388V, R262C, R62Q, M323V, E410K, D417H and D417N) into HeLa cells. The interaction of DCC with TUBB3 was assessed by co-immunoprecipitation (co-IP). Eight out of twelve *TUBB3* missense mutations (G82R, T178M, A302V, A302T, R262C, M323V, D417H and D417N) showed reductions in the interaction with DCC (Fig. 1A–C). To characterize which domain of TUBB3 interacts with DCC, wild type TUBB3, TUBB3-1-232 (a C-terminal truncation mutant) or TUBB3-233-449 (an N-terminal truncation mutant) cDNAs were co-transfected with DCC into HeLa cells. DCC could interact with TUBB3-233-449, but not TUBB3-1-232 (Fig. 1D). To further examine the interaction of endogenous DCC with TUBB3 missense mutants in primary neurons, we planned to transfect TUBB3 mutants A302V and R262C, two common mutant substitutions associated with defects in axon guidance and neuronal migration (Poirier et al., 2010; Tischfield et al., 2010), into E15 cortical neurons. To minimize the interference of endogenous TUBB3 on the interaction with DCC, several short hairpin based RNAi constructs (shRNAs) targeting 3’UTR of common human and mouse TUBB3 were designed

and transfected into primary E15 cortical neurons (Fig. 2A). Two shRNA constructs (#1 and #4) could significantly knock down the level of TUBB3 protein, whereas another (#6) could not (Fig. 2A). We used these RNAi constructs as TUBB3 shRNAs (combination of shRNAs #1 and #4) and TUBB3 control shRNA (#6), respectively. E15 cortical neurons were transfected with control shRNA, TUBB3 shRNAs, TUBB3 shRNAs plus either wild type TUBB3 or TUBB3 shRNA plus A302V or R262C. As expected, TUBB3 shRNAs dramatically knocked down endogenous TUBB3 (Fig. 2A–B). Expression of either A302V or R262C could restore TUBB3 protein levels in primary neurons after knockdown of endogenous TUBB3 compared to the wild type TUBB3 group (Fig. 2B).

TUBB3 colocalizes with DCC in the GC of primary cortical neurons (Qu et al., 2013a). To determine whether missense mutations in human *TUBB3* affect this colocalization, E15 mouse cortical neurons were nucleofected with TUBB3 shRNAs plus either wild type TUBB3 or two TUBB3 mutants, R262C and A302V. Quantitative colocalization analysis of confocal images showed partial overlap of immunofluorescent signals of DCC and wild type TUBB3 in the peripheral region of GCs (Fig. 2 C–E, quantification in Fig. 2L). However, expression of R262C or A302V decreased the overlap of DCC with these TUBB3 mutants (Fig. 2F–K, quantification in Fig. 2L). To rule out artificial overlaps of random signals, PCC value was recalculated after rotating one fluorescent channel of the same confocal image by 90 degrees (Shao et al., 2017; Tischfield et al., 2010). The PCC approximated zero in each group, indicating that the red and green signals are specifically correlated (Fig. 2M). These results suggest that TUBB3 mutations reduce the overlap of DCC with mutated TUBB3 proteins in the GC of primary cortical neurons. Interestingly, R262C and A302V appeared to mainly localize in the core region of the GC, whereas immunofluorescent signals of wild type TUBB3 widely distributed in the peripheral region of GC including lamellipodia and filopodia (Figs. 2D, 2G and 2J), suggesting that TUBB3 mutations may change intracellular distribution of mutated proteins (monomer mutated TUBB3 and/or polymerized TUBB3 in MTs) in the GC of primary neurons.

TUBB3 is strongly expressed in E15 cortical neurons (Huang et al., 2015; Qu et al., 2013a) and the disease-associated mutations in *TUBB3* could decrease the level of TUBB3 protein in brains (Tischfield et al., 2010). To mimic this reduction and minimize the interference of endogenous TUBB3 on the interaction with DCC with TUBB3 mutants, TUBB3 shRNAs were co-transfected with wild type TUBB3, R262C or A302V into primary E15 cortical neurons. Data from co-IP experiments indicated that netrin-1 increased the interaction of DCC with wild type TUBB3 (Fig. 3A–D), but not R262C (Fig. 3A and 3B) and A302V (Fig. 3C–D). Interestingly, expression of A302V alone in primary cortical neurons without knockdown of endogenous TUBB3 did not affect the interaction with DCC, but inhibited netrin-1 induced interaction of DCC with mutated TUBB3 (Fig. 3E–F). Altogether, these results suggest that A302V and R262C amino acid substitutions impaired the netrin-1-induced interaction of DCC with TUBB3. It is also possible that disruption of subcellular localization of mutated TUBB3 may prevent this interaction.

3.2. *TUBB3* mutations perturb netrin-1-induced interaction of DCC with polymerized TUBB3 in MTs

Coupling netrin-1/DCC signaling to MTs via polymerized TUBB3 is essential for netrin-1-mediated axon guidance (Qu et al., 2013a). To determine whether *TUBB3* mutations affect interaction of DCC with polymerized TUBB3, DCC-Myc was co-transfected with wild type human TUBB3-FLAG, R262C-FLAG or A302V-FLAG into HeLa cells and a co-sedimentation assay was performed as previously described (Fig. 4A–B) (Huang et al., 2015; Qu et al., 2013a; Shao et al., 2017). Cell lysates were incubated with taxol to stabilize MT against depolymerization under cold conditions. Monomerized TUBB3 subunits in the soluble supernatant (S) and polymerized TUBB3 in the pellet (P) were separated after centrifugation. The ratio of TUBB3 in P to S showed no significant difference among the wild type, A302V and R262C groups (Fig. 4A–B), suggesting that these mutants could be properly incorporated into MTs. However, expression of A302V and R262C inhibited the interaction of DCC with MTs with more DCC remained in the S than in the P compared to the wild type TUBB3 group (Fig. 4A–B). These data suggest that both A302V and R262C may alter the interaction of DCC with MTs. To further determine whether *TUBB3* mutations could interfere with netrin-1-induced interaction of endogenous DCC with polymerized TUBB3 in MTs, primary E15 cortical neurons were co-transfected with TUBB3 shRNAs plus wild type human TUBB3, A302V or R262C and stimulated with purified netrin-1 or sham-purified control. Cell lysates were treated with taxol *in vitro* to prevent polymerized MTs from depolymerization and a MT cosedimentation assay was performed. Without netrin-1, the P/S ratio of wild type TUBB3, A302V and R262C did not show any difference indicating that these mutants could be incorporated into MTs just like wild type TUBB3 (Fig. 4C–F). Netrin-1 stimulation could also increase P/S ratio of wild type TUBB3, R262C and A302V, suggesting that netrin-1 induced polymerization of these mutants into MTs (Fig. 4C–F). However, netrin-1 stimulation could not increase the P/S ratio of DCC in both A302V and R262C groups (Fig. 4C–F). As expected, netrin-1 induced the interaction of DCC with polymerized MTs in the wild type TUBB3 group (Fig. 4C–F). Altogether, these data indicate that A302V and R262C impair netrin-1-induced interaction of DCC with polymerized TUBB3 in MTs.

3.3. *TUBB3* mutations block netrin-1-induced neurite outgrowth

TUBB3 is required for netrin-1-induced neurite outgrowth (Qu et al., 2013a). To examine the functional role of *TUBB3* mutations in netrin signaling, constructs encoding Venus yellow fluorescent protein (Venus YFP) were cotransfected with control shRNA (Fig. 5A–B), TUBB3 shRNAs (Fig. 5C–D), TUBB3 shRNAs plus wild type TUBB3 (Fig. 5E–F), TUBB3 shRNAs plus R262C (Fig. 5G–H) or TUBB3 shRNA plus A302V (Fig. 5I–J) into E15 mouse cortical neurons as previously described (Huang et al., 2015; Li et al., 2008; Liu et al., 2004; Liu et al., 2007; Liu et al., 2009; Qu et al., 2013a; Qu et al., 2013b). Primary neurons were cultured in the presence of either netrin-1 or sham-purified control for 20 h. As reported previously (Qu et al., 2013a), netrin-1 promoted neurite outgrowth in neurons transfected with Venus YFP plus control shRNA, but not TUBB3 shRNAs (Figs. 5A–D and 5K). The expression of wild type human TUBB3 (Fig. 5E–F) (Qu et al., 2013a), but not R262C (Fig. 5G–H) or A302V (Fig. 5I–J), rescued the netrin-1-induced neurite outgrowth in neurons transfected with TUBB3 shRNAs (Fig. 5E–K). Basal axon outgrowth did not

change among the wild type, R262C and A302V groups (Fig. 5K). Interestingly, expression of either R262C or A302V alone in primary E15 cortical neurons without knocking down endogenous TUBB3 also inhibited netrin-1 induced neurite outgrowth (Fig. 6), suggesting that these missense mutations could function as dominant negative or gain-of-function regulators in netrin signaling. Altogether, these results indicate that R262C and A302V specifically block netrin-1-induced neurite outgrowth.

3.4. *TUBB3* mutations affect netrin-1-induced axon branching

Axon branching is a key event that allows neurons to interact with multiple synaptic targets to form functional neural circuits (Huang et al., 2015; Tymanskyj et al., 2017). Our previous work showed that TUBB3 is involved in netrin-1-induced axon branching (Huang et al., 2015). To examine whether *TUBB3* mutations disrupt this effect, mouse E15 cortical neurons were dissociated and nucleofected with Venus YFP together with control shRNA (Fig. 7A–B), TUBB3 shRNAs (Fig. 7C–D), TUBB3 shRNAs plus wild type TUBB3 (Fig. 7E–F), TUBB3 shRNAs plus A302V (Fig. 7G–H) or TUBB3 shRNAs plus R262C (Fig. 7I–J), respectively (Huang et al., 2015; Li et al., 2008; Liu et al., 2004; Liu et al., 2007; Liu et al., 2009; Qu et al., 2013a; Qu et al., 2013b). After transfection, primary neurons were cultured and stimulated with netrin-1 or sham-purified control for 72 h. As predicted, netrin-1 increased axon branching in the control shRNA-transfected neurons (Fig. 7A–B), but not in the TUBB3 shRNA-transfected neurons (Fig. 7C–D), and expression of wild type human TUBB3 (Fig. 7E–F) rescued the effect of TUBB3 knockdown on netrin-1-induced axon branching (quantification in Fig. 7K), which is consistent with our recent study (Huang et al., 2015). Importantly, netrin-1-promoted axon branching was dramatically inhibited in neurons transfected with TUBB3 shRNAs plus either A302V (Fig. 7G–H) or R262C (Fig. 7I–J, quantification in Fig. 7K). The induction of axon branching by netrin-1 was totally abolished in the A302V group, whereas expression of R262C could partially rescue netrin-1-induced axon branching after TUBB3 knockdown (Fig. 7K). In addition, expression of either R262C or A302V alone in primary cortical neurons without knockdown of endogenous TUBB3 also inhibited netrin-1-induced axon branching compared to the wild type TUBB3 group (Fig. 8). Altogether, these results indicate that *TUBB3* mutations disrupt netrin-1-induced axon branching.

3.5. *TUBB3* mutations inhibit netrin-1-promoted CA attraction

TUBB3 plays an important role in netrin-1-mediated axon attraction (Qu et al., 2013a). To determine whether *TUBB3* mutations specifically perturb netrin-1 attraction on spinal cord CAs, we performed an open book turning assay with CAs from the neural tube of chick embryos (Fig. 9A) as previously described (Li et al., 2008; Liu et al., 2004; Liu et al., 2007; Liu et al., 2009; Qu et al., 2013a). The Venus YFP construct plus wild type TUBB3, R262C or A302V were electroporated into the chick neural tube at stage 12–15. An explant of the neural tube was co-cultured with an aggregate of either control HEK cells or HEK cells stably secreting netrin-1 (Li et al., 2008; Liu et al., 2004; Liu et al., 2007; Liu et al., 2009; Qu et al., 2013a). Most CAs turned towards netrin-1 secreting HEK cells in explants transfected with Venus YFP together with wild type human TUBB3, whereas control HEK 293 cells could not attract CAs with most of axons projecting straight towards the floor plate (Fig. 9B–C, quantification in Fig. 9L). Co-transfection of Venus YFP with either R262C

(Fig. 9D–E) or A302V (Fig. 9F–G) did not affect axon turning in the control HEK cell group, but significantly inhibited axon turning towards netrin-1 secreting HEK cells (Fig. 9L). These results demonstrate that *TUBB3* mutations disrupt CA attraction induced by netrin-1.

3.6. *TUBB3* mutations impair spinal cord CA projection *in vivo*

To determine the functional role of *TUBB3* mutations *in vivo*, we examined CA projection in the developing chicken spinal cord (Li et al., 2008; Liu et al., 2004; Liu et al., 2007; Liu et al., 2009; Qu et al., 2013a; Qu et al., 2013b) (Fig. 10A). Venus YFP only (Fig. 10B), Venus YFP plus wild type human TUBB3 (Fig. 10C), Venus YFP plus A302V (Fig. 10D) or Venus YFP plus R262C (Fig. 10E) were introduced into the neural tube of chick embryos at stages 12–15 by *in ovo* electroporation (Li et al., 2008; Liu et al., 2004; Liu et al., 2007; Liu et al., 2009; Qu et al., 2013a). YFP-labeled chick spinal cords were collected at stage 23 and transverse sections of the lumbosacral segments of the spinal cord were prepared. In the neural tube transfected with Venus YFP alone (Fig. 10B) and Venus YFP plus the wild type TUBB3 (Fig. 10C), CAs projected normally toward the floor plate with most axons reaching the floor plate (quantification in Fig. 10F). In contrast, expression of either A302V or R262C not only inhibited CA projection, but caused axon misguidance (Figs. 10D–E and 10F–H). These findings indicate that TUBB3 mutations perturb spinal cord CA projection and pathfinding in the developing spinal cord.

4. Discussion

4.1. Missense mutations in *TUBB3* disrupt the interaction of DCC with polymerized TUBB3 in netrin signaling

Netrins are key guidance cues in the developing nervous system. Our recent data indicate that TUBB3, the highly dynamic β–tubulin isoform in neurons, directly links netrin-1/DCC signaling to MT dynamics and plays an important role in netrin-1-induced axon outgrowth, branching and attraction *in vitro* and spinal cord CA projection in the chicken embryo (Huang et al., 2015; Qu et al., 2013a). TUBB3 interacts directly with DCC and netrin-1 induces this interaction in primary neurons (Qu et al., 2013a). To reveal whether the disease-associated missense mutation in human *TUBB3* gene affects this interaction, either wild type TUBB3 or a single TUBB3 mutant was transfected into HeLa cells. Results from co-IP experiments indicate that the interaction of DCC with most of the TUBB3 mutants (8 out of 12) was reduced compared to the wild type TUBB3, suggesting that TUBB3 mutations may differentially disrupt the interaction with DCC (Fig. 1). As expected, DCC partially overlapped with TUBB3 in the P region of developing cortical neuron GCs (Fig. 2C–E) (Qu et al., 2013a). However, expression of either R262C or A302V, two common mutant substitutions associated with TUBB3 syndromes (Poirier et al., 2010; Tischfield et al., 2010), inhibited the colocalization of DCC with these mutants (Fig. 2). Netrin-1 dramatically increased the interaction of endogenous DCC with wild type TUBB3, but not R262C and A302V, in primary neurons (Fig. 3). Results from an MT cosedimentation assay demonstrated that DCC failed to interact with MTs containing polymerized R262C and A302V (Fig. 4). Expression of these mutants also blocked netrin-1-induced cosedimentation of DCC with stabilized MTs compared to the wild type TUBB3 (Fig. 4). Interestingly,

netrin-1 could still promote polymerization of R262C and A302V into MTs with more mutated proteins in the pellet than in the supernatant (Fig. 4). Altogether, these data suggest that TUBB3 mutations may disturb the coupling of netrin/DCC signaling with MT dynamics in the developing neurons.

DCC interacts with the C-terminal part of TUBB3 including the intermediate region and a C-terminal domain (Fig. 1D), which houses most of TUBB3 (9 out of 12) amino acid substitutions. The interaction of DCC with six of eight *TUBB3* missense mutations in these domains is significantly reduced compared to the wild type TUBB3 (Fig. 1), suggesting that *TUBB3* mutations may undergo a conformational change, disrupting the interaction with DCC. Previous studies suggested that TUBB3 substitutions distributed in the C-terminal, intermediate and N-terminal domains are implicated in modulation of MT dynamics and regulation of motor protein trafficking and interactions with microtubule associated proteins via affecting the tertiary protein structure (Li et al., 2002a; Lowe et al., 2001; Poirier et al., 2010; Tischfield et al., 2010). Netrin-1 increases the interaction of DCC with polymerized TUBB3 in MTs (Qu et al., 2013a; Shao et al., 2017). Both A302V and R262C disrupt the interaction of DCC with mutant MTs and impair netrin-1-induced interaction of DCC with polymerized TUBB3 in MTs (Fig. 4). These results suggest that missense mutations in human *TUBB3* could influence the conformation of TUBB3 protein and disturb the binding of DCC to both unpolymerized and polymerized TUBB3. We believe that it will be important to further characterize the mechanism underlying the interaction of DCC with specific TUBB3 mutants in netrin signaling.

4.2. *TUBB3* mutations specifically impair netrin-1-mediated axon outgrowth, branching and attraction

As a neuronal marker, TUBB3 is exclusively expressed in all neurons in the developing nervous system. However, missense mutations in the human *TUBB3* gene are associated with specific axon projection defects, such as impaired CA guidance (Poirier et al., 2010; Tischfield et al., 2010). To further determine whether *TUBB3* mutations specifically impair netrin signaling, the functional roles of R262C and A302V were studied by both *in vitro* and *in vivo* experiments. As previously reported (Huang et al., 2015; Qu et al., 2013a), TUBB3 shRNAs inhibited netrin-1-induced axon outgrowth (Fig. 5) and branching (Fig. 7) of cortical neurons compared to the control shRNA group. Expression of the wild-type human TUBB3, but not R262C or A302V, rescued the defects of TUBB3 knockdown in axon outgrowth and branching (Figs. 5 and 7). These results suggest that missense TUBB3 mutations may cause loss-of-function in netrin signaling. Interestingly, expression of either R262C or A302V alone in primary mouse cortical neurons without knockdown of endogenous TUBB3 also inhibited netrin-1-induced axon outgrowth (Fig. 6) and branching (Fig. 8). In addition, expression of either R262C or A302V inhibited netrin-1-induced axon attraction in the chicken ‘open-book’ turning assay (Fig. 9). The *in vivo* studies with the chick spinal cord showed that expression of R262C or A302V, but not wild type TUBB3, caused failure of CAs to reach the floor plate (Fig. 10), which is similar to defects of spinal cord CA projection observed in either *netrin-1*$^{-/-}$ or *DCC*$^{-/-}$ mice (Dominici et al., 2017; Fazeli et al., 1997; Serafini et al., 1996; Varadarajan et al., 2017). These findings suggest that mutant TUBB3 may also function as a dominant negative or gain-of function regulator

in netrin-mediated axon guidance. Altogether, these results indicate that missense *TUBB3* mutations may perturb netrin-1-mediated axon outgrowth, branching and attraction as well as CA projection and pathfinding in the developing spinal cord.

4.3. Potential roles of *TUBB* mutations in the signaling pathways downstream of netrin-1 and other guidance cues

Previous studies have shown that DCC collaborates with DSCAM mediating netrin-1-induced axon outgrowth and chemoattraction (Andrews et al., 2008; Liu et al., 2009; Ly et al., 2008), whereas interaction of UNC5 with DCC or DSCAM promotes axon repulsion (Finger et al., 2002; Hong et al., 1999; Purohit et al., 2012). Our recent work indicates that coordinated interaction of DCC and DSCAM with dynamic TUBB3 mediates netrin-1-induced axon branching (Huang et al., 2015). Interestingly, UNC5C also interacts with TUBB3 and uncoupling of UNC5C with polymerized TUBB3 in MTs mediates netrin-1 repulsion (Shao et al., 2017). Further investigation is necessary to untangle whether *TUBB3* mutations affect their binding to DSCAM and/or UNC5C and whether these mutants impair the coordination of DCC, DSCAM and UNC5C on modulation of MT dynamics in netrin signaling.

Interestingly, in the chicken genome, neogenin is the single identified orthologue of the mammalian neogenin and DCC genes. Previous studies suggested that chick neogenin could function as rodent DCC in guiding CA projection (Phan et al., 2011). Our results indicated that knockdown of TUBB3 or expression of either R262C or A302V in chicken spinal cords inhibited netrin-1-induced CA attraction *in vitro* (Fig. 9) and disrupted spinal cord CA projection *in vivo* (Fig. 10)(Qu et al., 2013a). It is likely that chicken neogenin may interact with TUBB3 and missense mutations in *TUBB3* could disrupt this interaction and impair netrin-1-mediated axon projection. This premise remains to be validated.

A variety of signaling molecules have been identified in netrin signaling, such as cyclic nucleotides (Song et al., 1997), phospholipase C (Ming et al., 1999), mitogen-activated protein kinases (Campbell and Holt, 2003; Forcet et al., 2002; Ming et al., 2002), phosphoinositol-3-kinase (Ming et al., 1999), transient receptor potential channels (Wang and Poo, 2005), calcium (Hong et al., 2000), the transcription factor NFAT (Graef et al., 2003) myosin-X (Zhu et al., 2007), metalloprotease(s), γ-secretase (Bai et al., 2011), and protein translation components (Tcherkezian et al., 2010). Netrin-1 stimulation recruits multiple signal transduction molecules, such as, Fyn, FAK, PAK1, $p130^{CAS}$, TRIO and DOCK180 through DCC to form a signaling complex (Li et al., 2004b; Liu et al., 2004; Meriane et al., 2004; Ren et al., 2004; Shekarabi et al., 2005), which then activates small GTPases Rac1 and Cdc42 (Briancon-Marjollet et al., 2008; Forsthoefel et al., 2005; Li et al., 2008; Li et al., 2002b; Liu et al., 2007; Shekarabi and Kennedy, 2002; Watari-Goshima et al., 2007) or inhibits RhoA in netrin-induced attraction (Moore et al., 2008). It remains to be determined whether the interaction of DCC with polymerized TUBB3 in MTs may function as a signaling platform to recruit signaling molecules in netrin-1-mediated attraction and *TUBB3* mutations disrupt formation of the signaling complex downstream netrin/DCC signaling.

Many extracellular signals including guidance cues, growth factors, and cell adhesion molecules, are involved in guiding GC navigation via modulation of cytoskeleton dynamics including filamentous actin and MTs (Dent et al., 2011; Guan and Rao, 2003; Kolodkin and Tessier-Lavigne, 2011; Lowery and Van Vactor, 2009; Stoeckli and Zou, 2009; Suh et al., 2004; Vitriol and Zheng, 2012). CA projections are guided by multiple guidance cues such as Sonic hedgehog (Charron et al., 2003), Wnt4 (Lyuksyutova et al., 2003), slits (Rothberg et al., 1990; Zou et al., 2000) and bone morphogenetic proteins (Augsburger et al., 1999; Butler and Dodd, 2003). Our biochemical data indicate that the disease-associated substitutions E205K, M388V, R62Q and E410K could interact with DCC that was similar to wild type TUBB3, while eight other TUBB3 mutants revealed a significant reduction of DCC binding (Fig. 1). Considering the phenotypic heterogeneity of *TUBB3* mutations, further investigation is needed to gain insight into the roles of *TUBB3* mutations in signaling mechanisms downstream of these guidance cues.

5. Conclusions

During embryonic development, modulation of MT dynamics in the GC of developing neurons is essential for proper axon outgrowth and projection. Direct coupling of netrin receptors with dynamic TUBB3 plays an important role in netrin-1-induced axon outgrowth, branching and attraction. Missense mutations in human *TUBB3* gene perturb MT dynamics, leading to brain malformation associated with axon guidance and neuronal migration defects. Our data have demonstrated that *TUBB3* mutations impair the interaction of DCC with polymerized TUBB3 in MTs and inhibits netrin-1-induced neurite outgrowth, branching and attraction. These results suggest a disease mechanism underlying *TUBB3* mutation-associated axon guidance defects: mutations in *TUBB3* disrupt engagement of netrin/DCC signaling with MT dynamics, resulting in specific defects of netrin-1-mediated axon projection in the developing nervous system.

Acknowledgments

We thank Dr. Jamel Chelly for TUBB3 mutants (G82R, T178M, E205K, M388V and A302V) and Dr. Elizabeth C Engle for TUBB3-V5 constructs. This work was supported by the National Institute of Health.

Abbreviations

DCC	deleted in colorectal cancer
DSCAM	Down syndrome cell adhesion molecule
UNC5	uncoordinated-5
CA	commissural axon
MT	microtubule
UTR	3' untranslated region
PAGE	polyacrylamide gel electrophoresis
PCC	Pearson Correlation Coefficient

ROI	region of interest
PFA	paraformaldehyde
co-IP	co-immunoprecipitation
YFP	yellow fluorescent protein

References

Abdollahi MR, Morrison E, Sirey T, Molnar Z, Hayward BE, Carr IM, Springell K, Woods CG, Ahmed M, Hattingh L, et al. Mutation of the variant alpha-tubulin TUBA8 results in polymicrogyria with optic nerve hypoplasia. Am J Hum Genet. 2009; 85:737–744. [PubMed: 19896110]

Ackerman SL, Kozak LP, Przyborski SA, Rund LA, Boyer BB, Knowles BB. The mouse rostral cerebellar malformation gene encodes an UNC-5-like protein. Nature. 1997; 386:838–842. [PubMed: 9126743]

Alcantara S, Ruiz M, De Castro F, Soriano E, Sotelo C. Netrin 1 acts as an attractive or as a repulsive cue for distinct migrating neurons during the development of the cerebellar system. Development. 2000; 127:1359–1372. [PubMed: 10704383]

Andrews GL, Tanglao S, Farmer WT, Morin S, Brotman S, Berberoglu MA, Price H, Fernandez GC, Mastick GS, Charron F, et al. Dscam guides embryonic axons by Netrin-dependent and -independent functions. Development. 2008; 135:3839–3848. [PubMed: 18948420]

Augsburger A, Schuchardt A, Hoskins S, Dodd J, Butler S. BMPs as mediators of roof plate repulsion of commissural neurons. Neuron. 1999; 24:127–141. [PubMed: 10677032]

Bai G, Chivatakarn O, Bonanomi D, Lettieri K, Franco L, Xia C, Stein E, Ma L, Lewcock JW, Pfaff SL. Presenilin-dependent receptor processing is required for axon guidance. Cell. 2011; 144:106–118. [PubMed: 21215373]

Briancon-Marjollet A, Ghogha A, Nawabi H, Triki I, Auziol C, Fromont S, Piche C, Enslen H, Chebli K, Cloutier JF, et al. Trio mediates netrin-1-induced Rac1 activation in axon outgrowth and guidance. Mol Cell Biol. 2008; 28:2314–2323. [PubMed: 18212043]

Buck KB, Zheng JQ. Growth cone turning induced by direct local modification of microtubule dynamics. J Neurosci. 2002; 22:9358–9367. [PubMed: 12417661]

Burgess RW, Jucius TJ, Ackerman SL. Motor axon guidance of the mammalian trochlear and phrenic nerves: dependence on the netrin receptor Unc5c and modifier loci. The Journal of neuroscience : the official journal of the Society for Neuroscience. 2006; 26:5756–5766. [PubMed: 16723533]

Butler SJ, Dodd J. A role for BMP heterodimers in roof plate-mediated repulsion of commissural axons. Neuron. 2003; 38:389–401. [PubMed: 12741987]

Campbell DS, Holt CE. Apoptotic pathway and MAPKs differentially regulate chemotropic responses of retinal growth cones. Neuron. 2003; 37:939–952. [PubMed: 12670423]

Challacombe JF, Snow DM, Letourneau PC. Dynamic microtubule ends are required for growth cone turning to avoid an inhibitory guidance cue. The Journal of neuroscience : the official journal of the Society for Neuroscience. 1997; 17:3085–3095. [PubMed: 9096143]

Charron F, Stein E, Jeong J, McMahon AP, Tessier-Lavigne M. The morphogen sonic hedgehog is an axonal chemoattractant that collaborates with netrin-1 in midline axon guidance. Cell. 2003; 113:11–23. [PubMed: 12679031]

Colamarino SA, Tessier-Lavigne M. The axonal chemoattractant netrin-1 is also a chemorepellent for trochlear motor axons. Cell. 1995; 81:621–629. [PubMed: 7758116]

Cushion TD, Dobyns WB, Mullins JGL, Stoodley N, Chung S-K, Fry AE, Hehr U, Gunny R, Aylsworth AS, Prabhakar P, et al. Overlapping cortical malformations and mutations in TUBB2B and TUBA1A. Brain. 2013; 136:536–548. [PubMed: 23361065]

Deiner MS, Kennedy TE, Fazeli A, Serafini T, Tessier-Lavigne M, Sretavan DW. Netrin-1 and DCC mediate axon guidance locally at the optic disc: loss of function leads to optic nerve hypoplasia. Neuron. 1997; 19:575–589. [PubMed: 9331350]

Dent EW, Barnes AM, Tang F, Kalil K. Netrin-1 and semaphorin 3A promote or inhibit cortical axon branching, respectively, by reorganization of the cytoskeleton. The Journal of neuroscience : the official journal of the Society for Neuroscience. 2004; 24:3002–3012. [PubMed: 15044539]

Dent EW, Gupton SL, Gertler FB. The growth cone cytoskeleton in axon outgrowth and guidance. Cold Spring Harbor perspectives in biology. 2011; 3

Dominici C, Moreno-Bravo JA, Puiggros SR, Rappeneau Q, Rama N, Vieugue P, Bernet A, Mehlen P, Chedotal A. Floor-plate-derived netrin-1 is dispensable for commissural axon guidance. Nature. 2017; 545:350–354. [PubMed: 28445456]

Fazeli A, Dickinson SL, Hermiston ML, Tighe RV, Steen RG, Small CG, Stoeckli ET, Keino-Masu K, Masu M, Rayburn H, et al. Phenotype of mice lacking functional Deleted in colorectal cancer (Dcc) gene. Nature. 1997; 386:796–804. [PubMed: 9126737]

Finger JH, Bronson RT, Harris B, Johnson K, Przyborski SA, Ackerman SL. The netrin 1 receptors Unc5h3 and Dcc are necessary at multiple choice points for the guidance of corticospinal tract axons. J Neurosci. 2002; 22:10346–10356. [PubMed: 12451134]

Fitzli D, Stoeckli ET, Kunz S, Siribour K, Rader C, Kunz B, Kozlov SV, Buchstaller A, Lane RP, Suter DM, et al. A direct interaction of axonin-1 with NgCAM-related cell adhesion molecule (NrCAM) results in guidance, but not growth of commissural axons. J Cell Biol. 2000; 149:951–968. [PubMed: 10811834]

Forcet C, Stein E, Pays L, Corset V, Llambi F, Tessier-Lavigne M, Mehlen P. Netrin-1-mediated axon outgrowth requires deleted in colorectal cancer-dependent MAPK activation. Nature. 2002; 417:443–447. [PubMed: 11986622]

Forsthoefel DJ, Liebl EC, Kolodziej PA, Seeger MA. The Abelson tyrosine kinase, the Trio GEF and Enabled interact with the Netrin receptor Frazzled in Drosophila. Development. 2005; 132:1983–1994. [PubMed: 15790972]

Graef IA, Wang F, Charron F, Chen L, Neilson J, Tessier-Lavigne M, Crabtree GR. Neurotrophins and netrins require calcineurin/NFAT signaling to stimulate outgrowth of embryonic axons. Cell. 2003; 113:657–670. [PubMed: 12787506]

Guan KL, Rao Y. Signalling mechanisms mediating neuronal responses to guidance cues. Nat Rev Neurosci. 2003; 4:941–956. [PubMed: 14682358]

Guerrini R, Mei D, Cordelli DM, Pucatti D, Franzoni E, Parrini E. Symmetric polymicrogyria and pachygyria associated with TUBB2B gene mutations. Eur J Hum Genet. 2012; 20:995–998. [PubMed: 22333901]

Hamburger V, Hamilton HL, Hamburger V, Hamilton HL. A series of normal stages in the development of the chick embryo. 1951. Developmental dynamics : an official publication of the American Association of Anatomists. 1992; 195:231–272. [PubMed: 1304821]

Hedgecock EM, Culotti JG, Hall DH. The unc-5, unc-6, and unc-40 genes guide circumferential migrations of pioneer axons and mesodermal cells on the epidermis in C. elegans. Neuron. 1990; 4:61–85. [PubMed: 2310575]

Hong K, Hinck L, Nishiyama M, Poo MM, Tessier-Lavigne M, Stein E. A ligand-gated association between cytoplasmic domains of UNC5 and DCC family receptors converts netrin-induced growth cone attraction to repulsion. Cell. 1999; 97:927–941. [PubMed: 10399920]

Hong K, Nishiyama M, Henley J, Tessier-Lavigne M, Poo M. Calcium signalling in the guidance of nerve growth by netrin-1. Nature. 2000; 403:93–98. [PubMed: 10638760]

Huang H, Shao Q, Qu C, Yang T, Dwyer T, Liu G. Coordinated interaction of Down syndrome cell adhesion molecule and deleted in colorectal cancer with dynamic TUBB3 mediates Netrin-1-induced axon branching. Neuroscience. 2015; 293:109–122. [PubMed: 25754961]

Ishii N, Wadsworth WG, Stern BD, Culotti JG, Hedgecock EM. UNC-6, a laminin-related protein, guides cell and pioneer axon migrations in C. elegans. Neuron. 1992; 9:873–881. [PubMed: 1329863]

Jaglin XH, Poirier K, Saillour Y, Buhler E, Tian G, Bahi-Buisson N, Fallet-Bianco C, Phan-Dinh-Tuy F, Kong XP, Bomont P, et al. Mutations in the beta-tubulin gene TUBB2B result in asymmetrical polymicrogyria. Nat Genet. 2009; 41:746–752. [PubMed: 19465910]

Kalil K, Dent EW. Touch and go: guidance cues signal to the growth cone cytoskeleton. Curr Opin Neurobiol. 2005; 15:521–526. [PubMed: 16143510]

Keeling SL, Gad JM, Cooper HM. Mouse Neogenin, a DCC-like molecule, has four splice variants and is expressed widely in the adult mouse and during embryogenesis. Oncogene. 1997; 15:691–700. [PubMed: 9264410]

Keino-Masu K, Masu M, Hinck L, Leonardo ED, Chan SS, Culotti JG, Tessier-Lavigne M. Deleted in Colorectal Cancer (DCC) encodes a netrin receptor. Cell. 1996; 87:175–185. [PubMed: 8861902]

Kennedy TE, Serafini T, de la Torre JR, Tessier-Lavigne M. Netrins are diffusible chemotropic factors for commissural axons in the embryonic spinal cord. Cell. 1994; 78:425–435. [PubMed: 8062385]

Kolodkin AL, Tessier-Lavigne M. Mechanisms and molecules of neuronal wiring: a primer. Cold Spring Harbor perspectives in biology. 2011; 3

Kolodziej PA, Timpe LC, Mitchell KJ, Fried SR, Goodman CS, Jan LY, Jan YN. frazzled encodes a Drosophila member of the DCC immunoglobulin subfamily and is required for CNS and motor axon guidance. Cell. 1996; 87:197–204. [PubMed: 8861904]

Kumar RA, Pilz DT, Babatz TD, Cushion TD, Harvey K, Topf M, Yates L, Robb S, Uyanik G, Mancini GMS. TUBA1A mutations cause wide spectrum lissencephaly (smooth brain) and suggest that multiple neuronal migration pathways converge on alpha tubulins. Human molecular genetics. 2010; 19:2817–2827. [PubMed: 20466733]

Lee AC, Suter DM. Quantitative analysis of microtubule dynamics during adhesion-mediated growth cone guidance. Dev Neurobiol. 2008; 68:1363–1377. [PubMed: 18698606]

Lei WL, Xing SG, Deng CY, Ju XC, Jiang XY, Luo ZG. Laminin/beta1 integrin signal triggers axon formation by promoting microtubule assembly and stabilization. Cell Res. 2012; 22:954–972. [PubMed: 22430151]

Leonardo ED, Hinck L, Masu M, Keino-Masu K, Ackerman SL, Tessier-Lavigne M. Vertebrate homologues of C. elegans UNC-5 are candidate netrin receptors. Nature. 1997; 386:833–838. [PubMed: 9126742]

Li H, DeRosier DJ, Nicholson WV, Nogales E, Downing KH. Microtubule structure at 8 A resolution. Structure. 2002a; 10:1317–1328. [PubMed: 12377118]

Li W, Lee J, Vikis HG, Lee S-H, Liu G, Aurandt J, Shen T-L, Fearon ER, Guan J-L, Han M, et al. Activation of FAK and Src are receptor-proximal events required for netrin signaling. Nature neuroscience. 2004a; 7:1213–1221. [PubMed: 15494734]

Li W, Lee J, Vikis HG, Lee SH, Liu G, Aurandt J, Shen TL, Fearon ER, Guan JL, Han M, et al. Activation of FAK and Src are receptor-proximal events required for netrin signaling. Nat Neurosci. 2004b; 7:1213–1221. [PubMed: 15494734]

Li X, Gao X, Liu G, Xiong W, Wu J, Rao Y. Netrin signal transduction and the guanine nucleotide exchange factor DOCK180 in attractive signaling. Nat Neurosci. 2008; 11:28–35. [PubMed: 18066058]

Li X, Saint-Cyr-Proulx E, Aktories K, Lamarche-Vane N. Rac1 and Cdc42 but not RhoA or Rho kinase activities are required for neurite outgrowth induced by the Netrin-1 receptor DCC (deleted in colorectal cancer) in N1E-115 neuroblastoma cells. J Biol Chem. 2002b; 277:15207–15214. [PubMed: 11844789]

Liu G, Beggs H, Jurgensen C, Park HT, Tang H, Gorski J, Jones KR, Reichardt LF, Wu J, Rao Y. Netrin requires focal adhesion kinase and Src family kinases for axon outgrowth and attraction. Nat Neurosci. 2004; 7:1222–1232. [PubMed: 15494732]

Liu G, Dwyer T. Microtubule dynamics in axon guidance. Neuroscience bulletin. 2014; 30:569–583. [PubMed: 24968808]

Liu G, Li W, Gao X, Li X, Jurgensen C, Park HT, Shin NY, Yu J, He ML, Hanks SK, et al. p130CAS is required for netrin signaling and commissural axon guidance. J Neurosci. 2007; 27:957–968. [PubMed: 17251438]

Liu G, Li W, Wang L, Kar A, Guan KL, Rao Y, Wu JY. DSCAM functions as a netrin receptor in commissural axon pathfinding. Proc Natl Acad Sci U S A. 2009; 106:2951–2956. [PubMed: 19196994]

Lowe J, Li H, Downing KH, Nogales E. Refined structure of alpha beta-tubulin at 3.5 A resolution. J Mol Biol. 2001; 313:1045–1057. [PubMed: 11700061]

Lowery LA, Van Vactor D. The trip of the tip: understanding the growth cone machinery. Nat Rev Mol Cell Biol. 2009; 10:332–343. [PubMed: 19373241]

Ly A, Nikolaev A, Suresh G, Zheng Y, Tessier-Lavigne M, Stein E. DSCAM is a netrin receptor that collaborates with DCC in mediating turning responses to netrin-1. Cell. 2008; 133:1241–1254. [PubMed: 18585357]

Lyuksyutova AI, Lu C-C, Milanesio N, King LA, Guo N, Wang Y, Nathans J, Tessier-Lavigne M, Zou Y. Anterior-posterior guidance of commissural axons by Wnt-frizzled signaling. Science (New York, N Y). 2003; 302:1984–1988.

Meriane M, Tcherkezian J, Webber CA, Danek EI, Triki I, McFarlane S, Bloch-Gallego E, Lamarche-Vane N. Phosphorylation of DCC by Fyn mediates Netrin-1 signaling in growth cone guidance. J Cell Biol. 2004; 167:687–698. [PubMed: 15557120]

Ming G, Song H, Berninger B, Inagaki N, Tessier-Lavigne M, Poo M. Phospholipase C-gamma and phosphoinositide 3-kinase mediate cytoplasmic signaling in nerve growth cone guidance. Neuron. 1999; 23:139–148. [PubMed: 10402200]

Ming GL, Wong ST, Henley J, Yuan XB, Song HJ, Spitzer NC, Poo MM. Adaptation in the chemotactic guidance of nerve growth cones. Nature. 2002; 417:411–418. [PubMed: 11986620]

Moore SW, Correia JP, Lai Wing Sun K, Pool M, Fournier AE, Kennedy TE. Rho inhibition recruits DCC to the neuronal plasma membrane and enhances axon chemoattraction to netrin 1. Development. 2008; 135:2855–2864. [PubMed: 18653556]

Phan KD, Croteau LP, Kam JW, Kania A, Cloutier JF, Butler SJ. Neogenin may functionally substitute for Dcc in chicken. PLoS One. 2011; 6:e22072. [PubMed: 21779375]

Poirier K, Saillour Y, Bahi-Buisson N, Jaglin XH, Fallet-Bianco C, Nabbout R, Castelnau-Ptakhine L, Roubertie A, Attie-Bitach T, Desguerre I, et al. Mutations in the neuronal ss-tubulin subunit TUBB3 result in malformation of cortical development and neuronal migration defects. Hum Mol Genet. 2010; 19:4462–4473. [PubMed: 20829227]

Purohit AA, Li W, Qu C, Dwyer T, Shao Q, Guan K-L, Liu G. Down syndrome cell adhesion molecule (DSCAM) associates with uncoordinated-5C (UNC5C) in netrin-1-mediated growth cone collapse. The Journal of biological chemistry. 2012; 287:27126–27138. [PubMed: 22685302]

Purro SA, Ciani L, Hoyos-Flight M, Stamatakou E, Siomou E, Salinas PC. Wnt regulates axon behavior through changes in microtubule growth directionality: a new role for adenomatous polyposis coli. The Journal of neuroscience : the official journal of the Society for Neuroscience. 2008; 28:8644–8654. [PubMed: 18716223]

Qu C, Dwyer T, Shao Q, Yang T, Huang H, Liu G. Direct binding of TUBB3 with DCC couples netrin-1 signaling to intracellular microtubule dynamics in axon outgrowth and guidance. J Cell Sci. 2013a; 126:3070–3081. [PubMed: 23641072]

Qu C, Li W, Shao Q, Dwyer T, Huang H, Yang T, Liu G. c-Jun N-terminal kinase 1 (JNK1) is required for coordination of netrin signaling in axon guidance. J Biol Chem. 2013b; 288:1883–1895. [PubMed: 23223444]

Ren XR, Ming GL, Xie Y, Hong Y, Sun DM, Zhao ZQ, Feng Z, Wang Q, Shim S, Chen ZF, et al. Focal adhesion kinase in netrin-1 signaling. Nat Neurosci. 2004; 7:1204–1212. [PubMed: 15494733]

Rothberg JM, Jacobs JR, Goodman CS, Artavanis-Tsakonas S. slit: an extracellular protein necessary for development of midline glia and commissural axon pathways contains both EGF and LRR domains. Genes Dev. 1990; 4:2169–2187. [PubMed: 2176636]

Sabry JH, O'Connor TP, Evans L, Toroian-Raymond A, Kirschner M, Bentley D. Microtubule behavior during guidance of pioneer neuron growth cones in situ. J Cell Biol. 1991; 115:381–395. [PubMed: 1918146]

Serafini T, Colamarino SA, Leonardo ED, Wang H, Beddington R, Skarnes WC, Tessier-Lavigne M. Netrin-1 is required for commissural axon guidance in the developing vertebrate nervous system. Cell. 1996; 87:1001–1014. [PubMed: 8978605]

Shao Q, Yang T, Huang H, Alarmanazi F, Liu G. Uncoupling of UNC5C with Polymerized TUBB3 in Microtubules Mediates Netrin-1 Repulsion. J Neurosci. 2017; 37:5620–5633. [PubMed: 28483977]

Shekarabi M, Kennedy TE. The netrin-1 receptor DCC promotes filopodia formation and cell spreading by activating Cdc42 and Rac1. Mol Cell Neurosci. 2002; 19:1–17. [PubMed: 11817894]

Shekarabi M, Moore SW, Tritsch NX, Morris SJ, Bouchard JF, Kennedy TE. Deleted in colorectal cancer binding netrin-1 mediates cell substrate adhesion and recruits Cdc42, Rac1, Pak1, and N-

WASP into an intracellular signaling complex that promotes growth cone expansion. J Neurosci. 2005; 25:3132–3141. [PubMed: 15788770]

Song HJ, Ming GL, Poo MM. cAMP-induced switching in turning direction of nerve growth cones. Nature. 1997; 388:275–279. [PubMed: 9230436]

Stoeckli E, Zou Y. How are neurons wired to form functional and plastic circuits? Meeting on Axon Guidance, Synaptogenesis & Neural Plasticity. EMBO Rep. 2009; 10:326–330. [PubMed: 19305387]

Stoeckli ET, Sonderegger P, Pollerberg GE, Landmesser LT. Interference with axonin-1 and NrCAM interactions unmasks a floor-plate activity inhibitory for commissural axons. Neuron. 1997; 18:209–221. [PubMed: 9052792]

Suh LH, Oster SF, Soehrman SS, Grenningloh G, Sretavan DW. L1/Laminin modulation of growth cone response to EphB triggers growth pauses and regulates the microtubule destabilizing protein SCG10. J Neurosci. 2004; 24:1976–1986. [PubMed: 14985440]

Tanaka E, Ho T, Kirschner MW. The role of microtubule dynamics in growth cone motility and axonal growth. J Cell Biol. 1995; 128:139–155. [PubMed: 7822411]

Tcherkezian J, Brittis PA, Thomas F, Roux PP, Flanagan JG. Transmembrane receptor DCC associates with protein synthesis machinery and regulates translation. Cell. 2010; 141:632–644. [PubMed: 20434207]

Tessier-Lavigne M, Placzek M, Lumsden AG, Dodd J, Jessell TM. Chemotropic guidance of developing axons in the mammalian central nervous system. Nature. 1988; 336:775–778. [PubMed: 3205306]

Tischfield MA, Baris HN, Wu C, Rudolph G, Van Maldergem L, He W, Chan WM, Andrews C, Demer JL, Robertson RL, et al. Human TUBB3 mutations perturb microtubule dynamics, kinesin interactions, and axon guidance. Cell. 2010; 140:74–87. [PubMed: 20074521]

Tischfield MA, Cederquist GY, Gupta ML Jr, Engle EC. Phenotypic spectrum of the tubulin-related disorders and functional implications of disease-causing mutations. Curr Opin Genet Dev. 2011; 21:286–294. [PubMed: 21292473]

Tymanskyj SR, Yang B, Falnikar A, Lepore AC, Ma L. MAP7 Regulates Axon Collateral Branch Development in Dorsal Root Ganglion Neurons. J Neurosci. 2017; 37:1648–1661. [PubMed: 28069923]

Varadarajan SG, Kong JH, Phan KD, Kao TJ, Panaitof SC, Cardin J, Eltzschig H, Kania A, Novitch BG, Butler SJ. Netrin1 Produced by Neural Progenitors, Not Floor Plate Cells, Is Required for Axon Guidance in the Spinal Cord. Neuron. 2017; 94:790–799. e793. [PubMed: 28434801]

Vitriol EA, Zheng JQ. Growth cone travel in space and time: the cellular ensemble of cytoskeleton, adhesion, and membrane. Neuron. 2012; 73:1068–1081. [PubMed: 22445336]

Wang GX, Poo MM. Requirement of TRPC channels in netrin-1-induced chemotropic turning of nerve growth cones. Nature. 2005; 434:898–904. [PubMed: 15758951]

Watari-Goshima N, Ogura K, Wolf FW, Goshima Y, Garriga G. C. elegans VAB-8 and UNC-73 regulate the SAX-3 receptor to direct cell and growth-cone migrations. Nat Neurosci. 2007; 10:169–176. [PubMed: 17237778]

Zhu XJ, Wang CZ, Dai PG, Xie Y, Song NN, Liu Y, Du QS, Mei L, Ding YQ, Xiong WC. Myosin X regulates netrin receptors and functions in axonal path-finding. Nat Cell Biol. 2007; 9:184–192. [PubMed: 17237772]

Zou Y, Stoeckli E, Chen H, Tessier-Lavigne M. Squeezing axons out of the gray matter: a role for slit and semaphorin proteins from midline and ventral spinal cord. Cell. 2000; 102:363–375. [PubMed: 10975526]

Highlights

Note: DCC, deleted in colorectal cancer; MTs, microtubules

- *TUBB3* mutations impair the interaction of DCC with TUBB3.
- *TUBB3* mutations perturb netrin-1-induced interaction of DCC with polymerized TUBB3 in MTs.
- *TUBB3* mutations block netrin-1-induced neurite outgrowth and branching.
- *TUBB3* mutations inhibit netrin-1-promoted commissural axon attraction.
- *TUBB3* mutations impair spinal cord commissural axon projection *in vivo*.

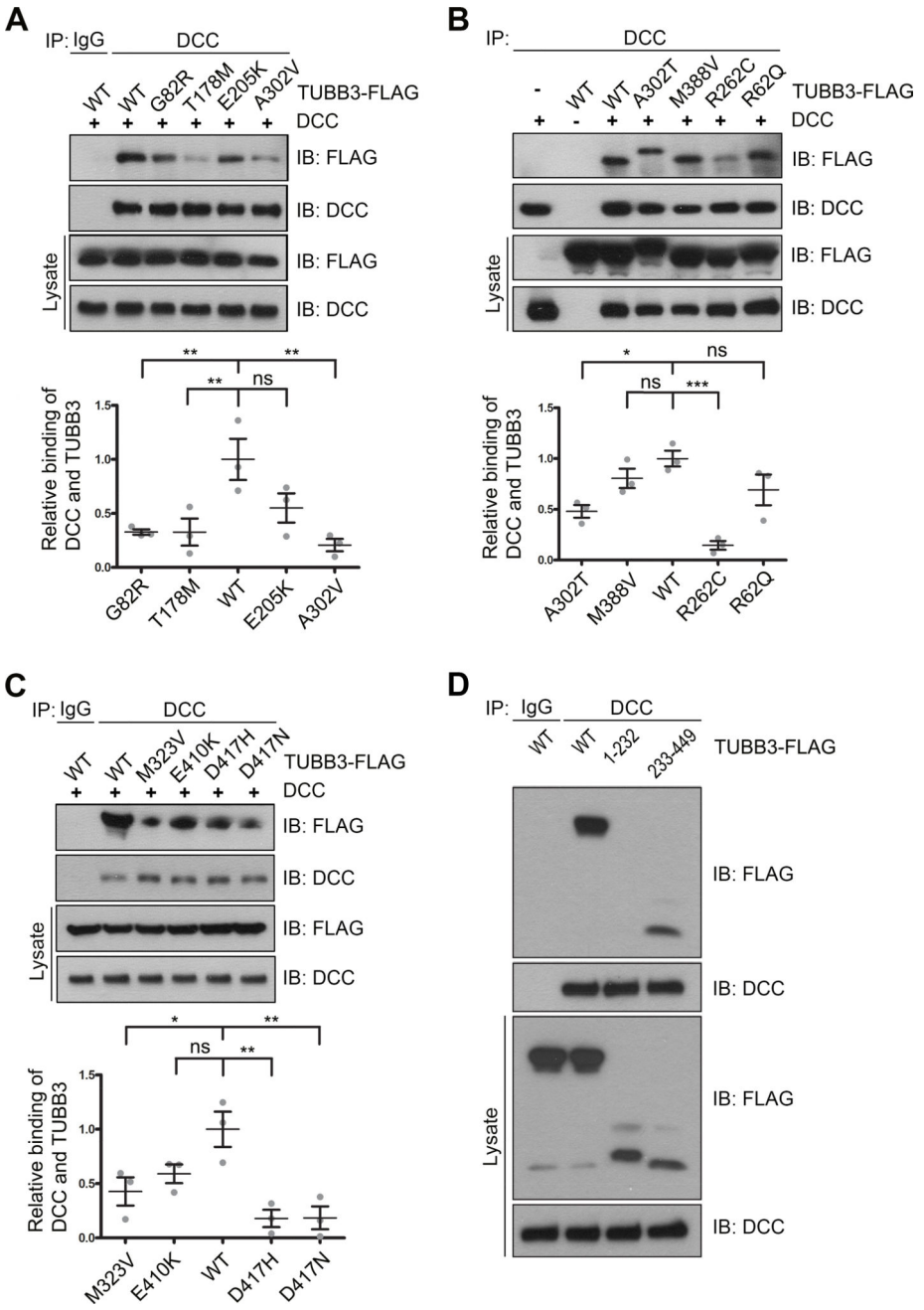

Figure 1.

Interaction of DCC with TUBB3 mutants. HeLa cells were transfected with human full-length DCC-Myc plus wild type human TUBB3 (A–D) or FLAG-tagged TUBB3 mutants (G82R, T178M, E205K and A302V in A, A302T, M388V, R262C and R62Q in B, M323V, E410K, D417H and D417N in C, and truncation mutants TUBB3-1-232 and TUBB3-233-449 in D, respectively). The anti-DCC antibody was used to immunoprecipitate DCC and the blot analyzed with anti-FLAG and anti-DCC antibodies. Relative binding of DCC to TUBB3 in A, B and C was quantified in the corresponding lower panel. The Y axis is the normalized ratio of mean intensity (arbitrary units) of FLAG to DCC. Data are mean ±

s.e.m from three separate experiments. *p<0.05, **p<0.01, ***p<0.0001, ns, no significant difference (one-way Anova and Tukey's test for post-hoc comparsions).

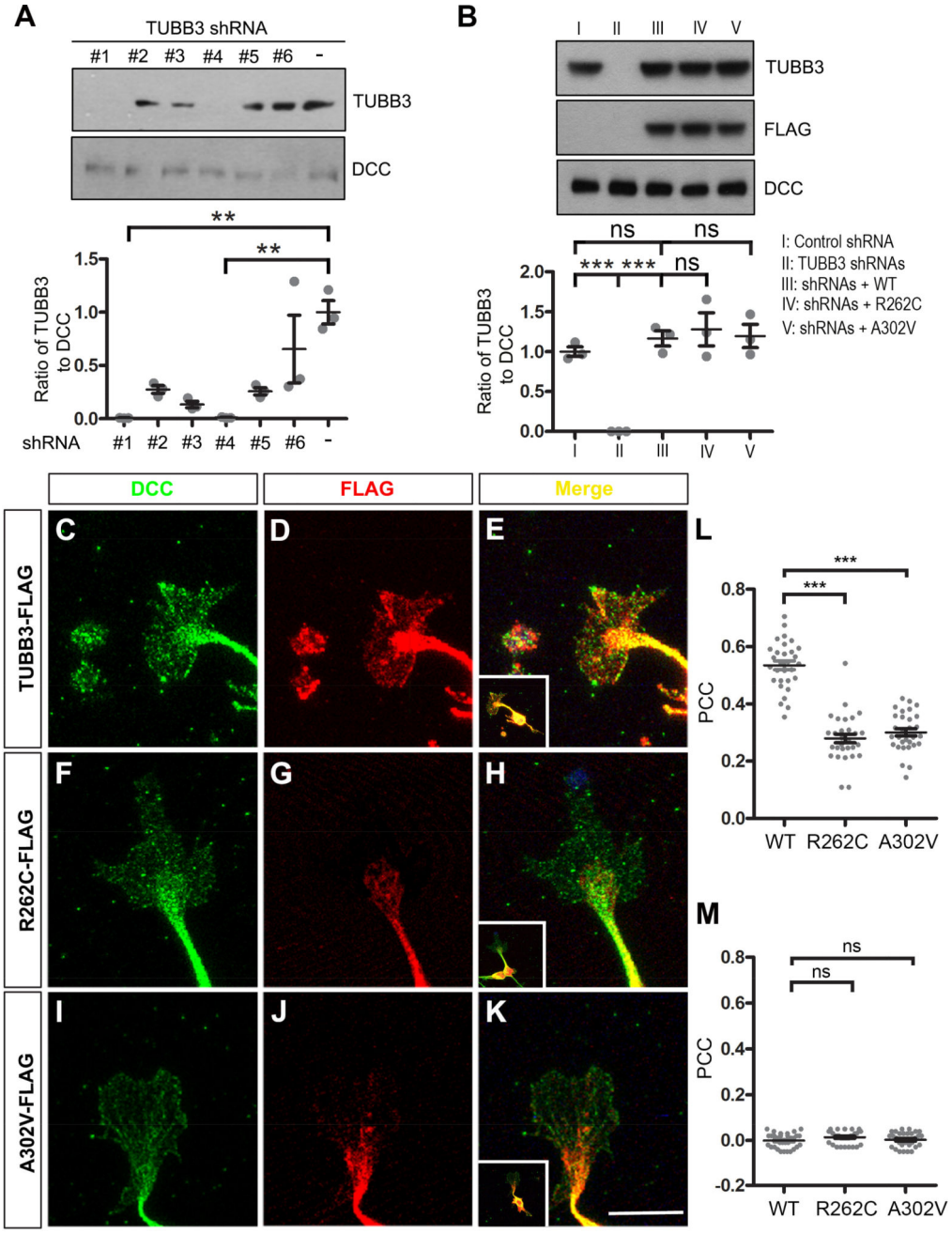

Figure 2.

TUBB3 mutations reduce the subcellular overlap of DCC with TUBB3 in the GC of primary neurons. A. Knockdown of endogenous TUBB3 in primary neurons. E15 mouse cortical neurons were nucleofected with several shRNAs targeting 3'UTR of human and mouse TUBB3. shRNA #1 and #4 dramatically reduced endogenous TUBB3 protein levels. ** indicates $p<0.01$ (one-way Anova and Tukey's test for post-hoc comparsions). B. Expression of wild type human TUBB3, R262C and A302V could restore TUBB3 protein levels after knockdown of endogenous TUBB3. E15 cortical neurons were transfected with control shRNA, TUBB3 shRNAs (#1 and #4), TUBB3 shRNAs (#1 and #4) plus wild type human

TUBB3, TUBB3 shRNAs (#1 and #4) plus R262C, or TUBB3 shRNAs (#1 and #4) plus A302V, respectively. TUBB3 and DCC were examined by Western blotting. C–K. TUBB3 shRNAs were co-transfected with the wild type human TUBB3 (C–E), R262C (F–H) or A302V (I–K) into mouse E15 cortical neurons. Primary neurons were cultured for 2 days and immunostained with anti-DCC and anti-FLAG antibodies. E, H and K are the merged images of C and D, F and G, and I and J, respectively. Scale bar: 10μm. L. Quantitative analysis of PCC in the ROI of the GC. The value of PCC in C–E, F–H, and I–K is 0.53 ± 0.08, 0.28 ± 0.08, and 0.3 ± 0.07, respectively. 30 GCs in each group were analyzed. *** indicates $p<0.0001$ (one-way Anova and Tukey's test for post-hoc comparisons). M. Analysis of PCC in the ROI of the GC after 90 degree counterclockwise rotation of the red fluorescence channel. ns indicates no significant difference (one-way Anova and Tukey's test for post-hoc comparisons).

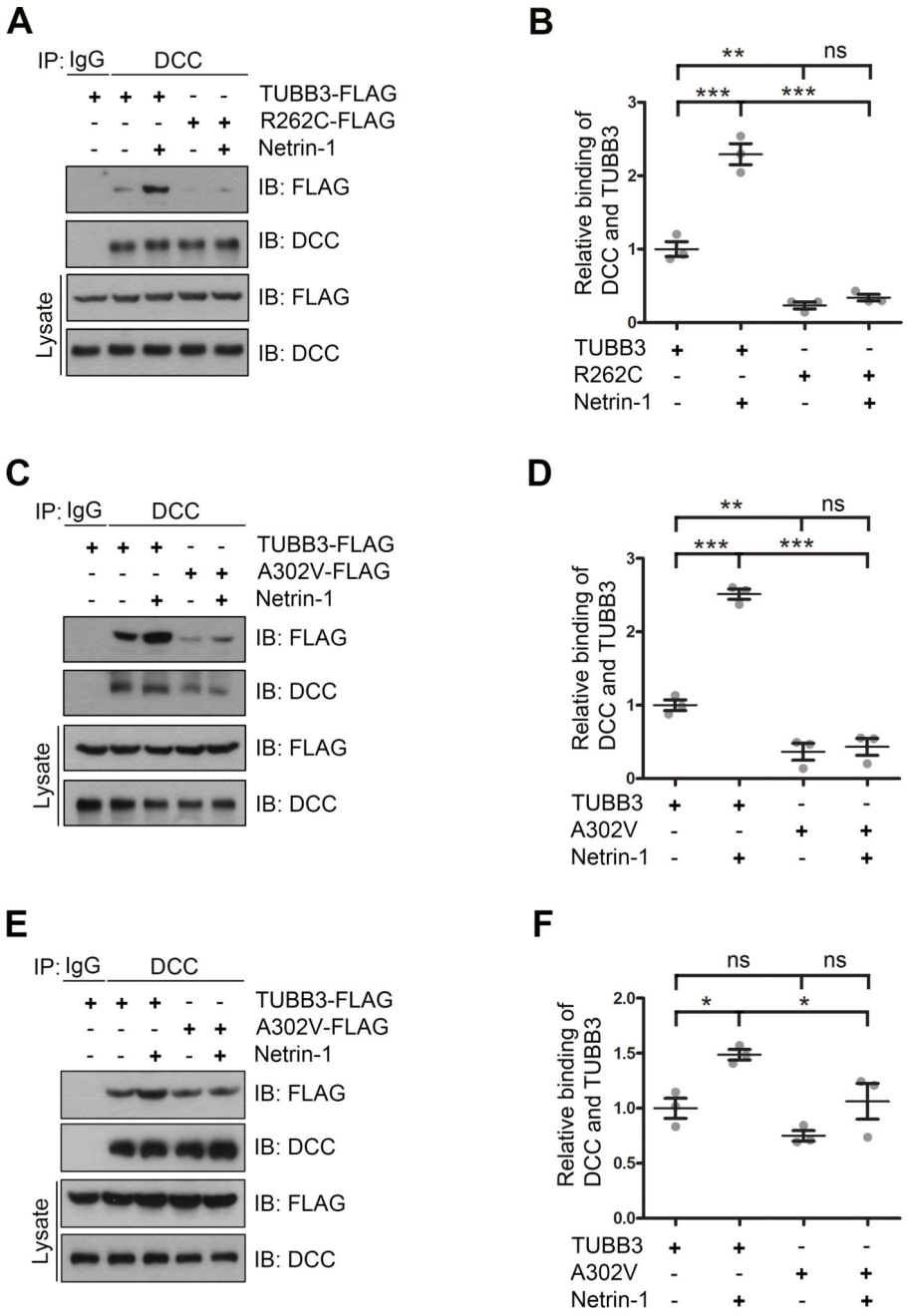

Figure 3.

TUBB3 mutations inhibit netrin-1-induced interaction of DCC with TUBB3. A–D. TUBB3 shRNAs were co-transfected with wild type human TUBB3 (A–D), R262C (A and B) or A302V (C and D) into mouse E15 cortical neurons. E–F. Mouse E15 cortical neurons were transfected with either wild type human TUBB3 or A302V. Primary neurons were cultured overnight and stimulated with purified netrin-1 or sham-purified control for 20 min. Cell lysates were immunoprecipitated with anti-DCC and followed by probing with anti-DCC, anti-FLAG antibodies. B, D and F. Quantification of relative binding of DCC to TUBB3-FLAG (B, D and F), R262C-FLAG (B) and A302V-FLAG (D and F). The Y axis is the

normalized ratio of mean intensity (arbitrary units) of FLAG to DCC. Data are mean ± s.e.m from three separate experiments. *p<0.05, **p<0.01, ***p<0.0001, ns indicates no significant difference (one-way Anova and Tukey's test for post-hoc comparsions).

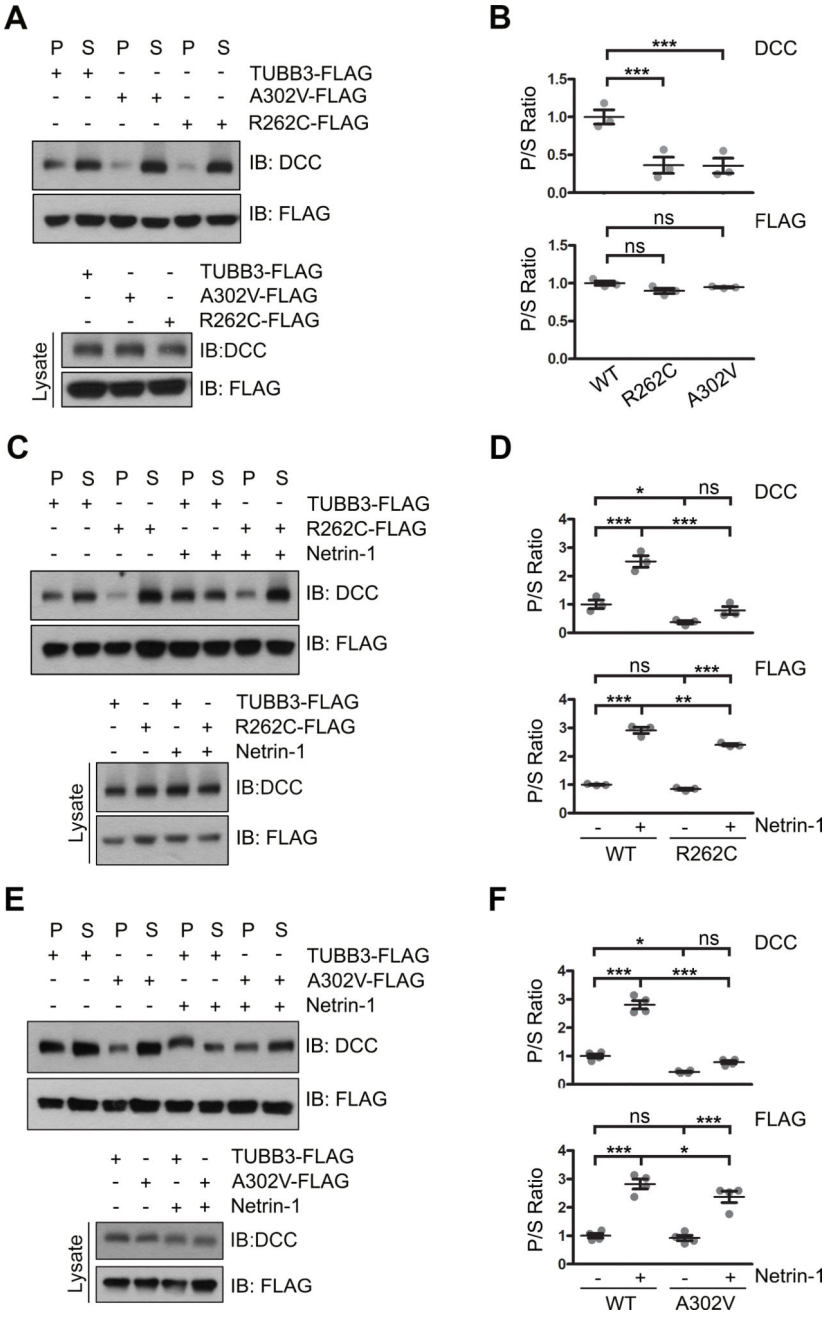

Figure 4.

TUBB3 mutations decrease the interaction of DCC with polymerized TUBB3 mutants. A. DCC was cotransfected with wild type human TUBB3, R262C or A302V into HeLa cells and a cosedimentation assay was performed. DCC and TUBB3 proteins in the pellet (P) and supernatant (S) fractions were analyzed by immunoblotting using anti-DCC and anti-FLAG antibodies, respectively. B. Quantification of P/S ratio of DCC and TUBB3 in A (three independent experiments). *** indicates $p<0.0001$, ns indicates no significant difference (one-way Anova and Tukey's test for post-hoc comparisons). C-F. TUBB3 shRNAs were co-transfected with wild type TUBB3 (C–F), R262C (C and D) or A302V (E and F) into mouse

E15 cortical neurons. Primary neurons were stimulated with purified netrin-1 or sham-purified control. The co-sedimentation assay of cell lysates was conducted with taxol to stabilize MTs *in vitro*. DCC and TUBB3-FLAG in the P and S fractions were examined by Western blotting. D and F are quantification of P/S ratio of DCC and TUBB3 in C and E, respectively. Data are mean ± s.e.m from three separate experiments. *$p<0.05$, **$p<0.01$, ***$p<0.001$, ns indicates no significant difference (one-way Anova and Tukey's test for post-hoc comparisons). WT, wild type human TUBB3-FLAG.

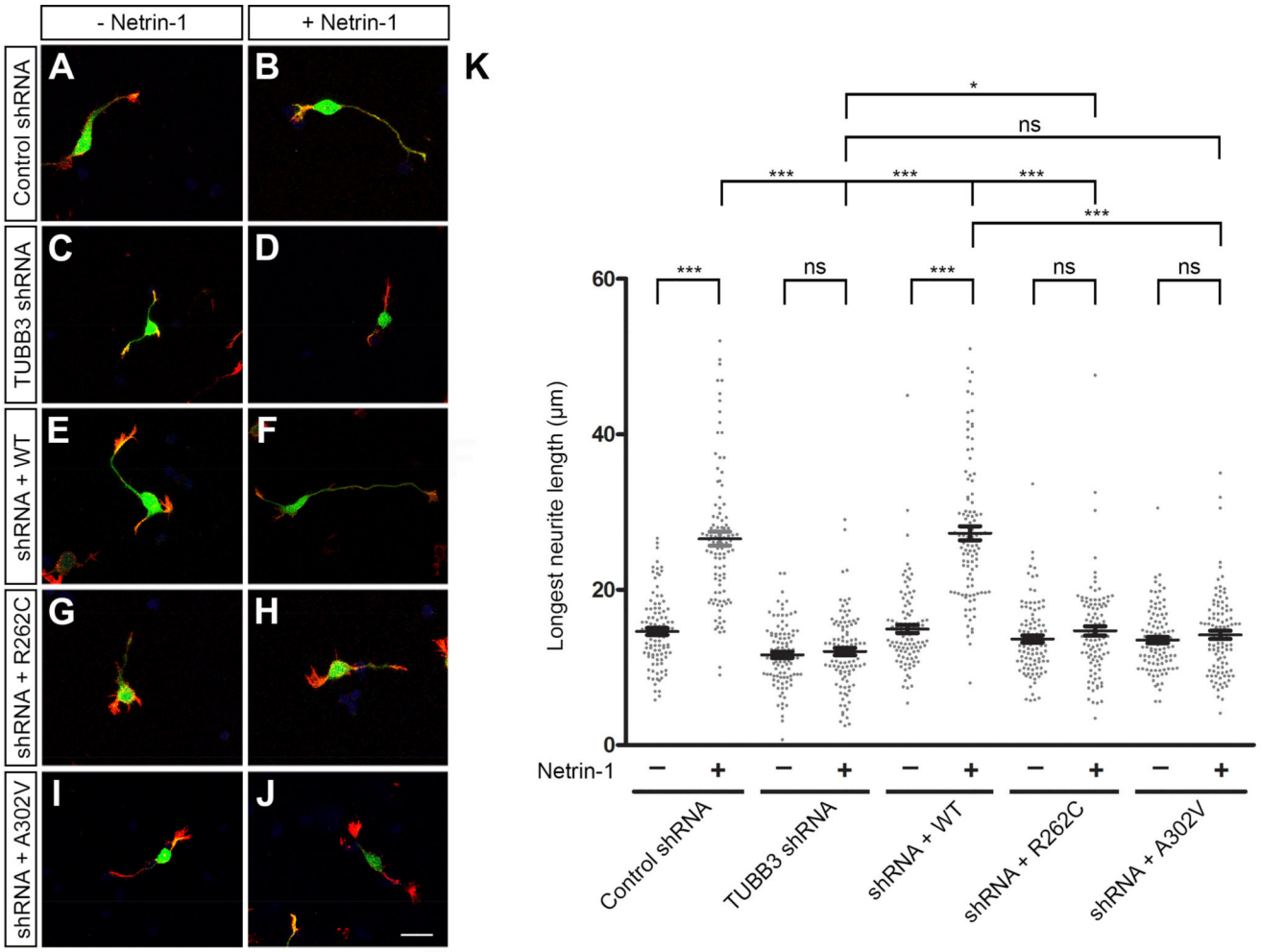

Figure 5.

TUBB3 mutations inhibit netrin-1-induced neurite outgrowth of cortical neurons. A–J. Venus YFP was co-transfected with TUBB3 control shRNA (A and B), TUBB3 shRNAs (C and D), TUBB3 shRNAs plus the wild type human TUBB3 (E and F), TUBB3 shRNAs plus R262C (G and H) or TUBB3 shRNAs plus A302V (I AND J), into E15 cortical neurons. Primary neurons were incubated with purified netrin-1 (B, D, F, H and J) or sham-purified control (A, C, E, G and I) for 20 h and stained with Alexa Fluor® 555 phalloidin (red) and DAPI (blue). Scale bar, 10 μm. (K) Quantification of netrin-1-induced neurite outgrowth. The Y axis is the longest neurite length per neuron. Data are mean ± s.e.m. 100 neurons/group from three independent experiments were analyzed. *p<0.05, ***p<0.0001, ns indicates no significant difference (one-way Anova and Tukey's test for post-hoc comparisons).

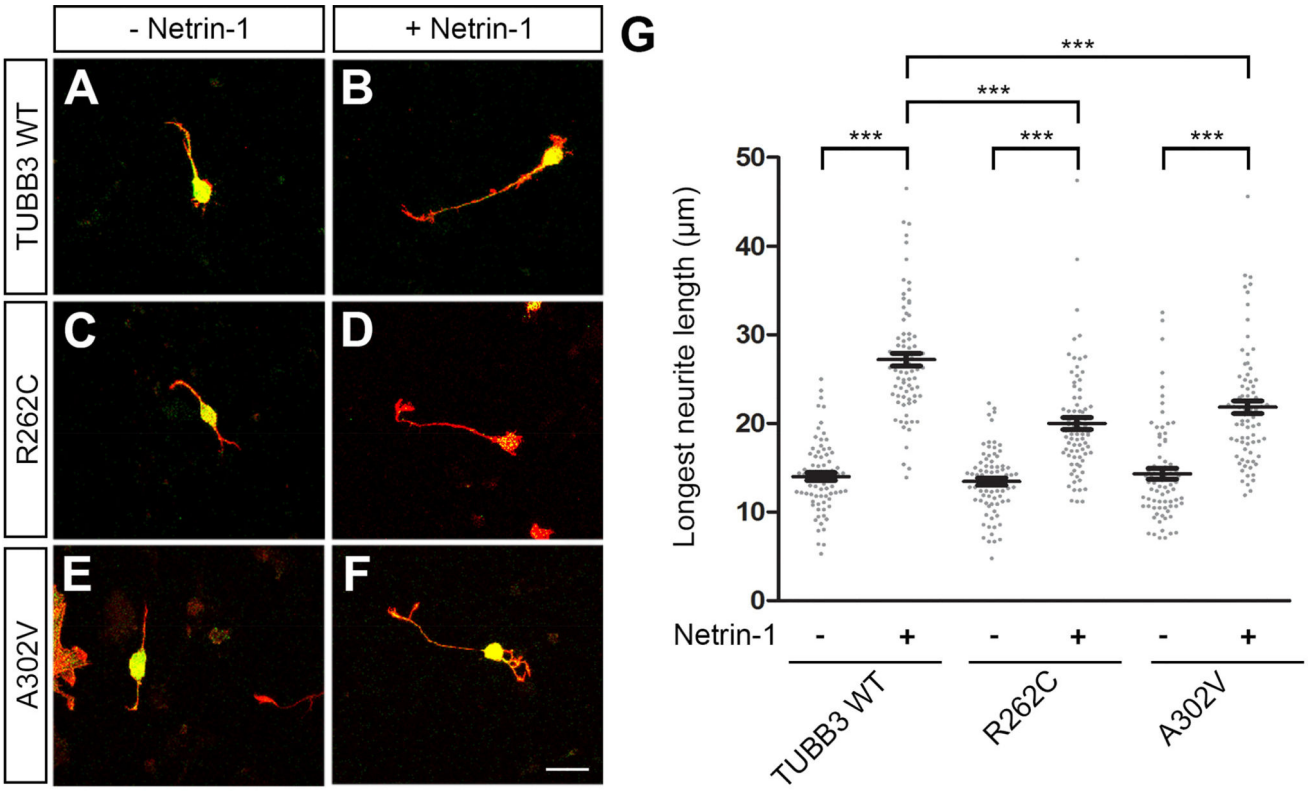

Figure 6.

Expression of either R262C or A302V in cortical neurons without knockdown of endogenous TUBB3 inhibits netrin-1-induced neurite outgrowth. Venus YFP was co-transfected with the wild type human TUBB3 (A and B), R262C (C and D) or A302V (E and F) into E15 cortical neurons. Primary neurons after transfection were incubated with purified netrin-1 (B, D and F) or sham-purified control (A, C and E) for 20 h and stained with Alexa Fluor® 555 phalloidin (red) and DAPI (blue). Scale bar, 10 μm. (G) Quantification of netrin-1-induced neurite outgrowth. Data are mean ± s.e.m. 79 neurons/group from three independent experiments were analyzed. ***$p<0.0001$ (one-way Anova and Tukey's test for post-hoc comparisons).

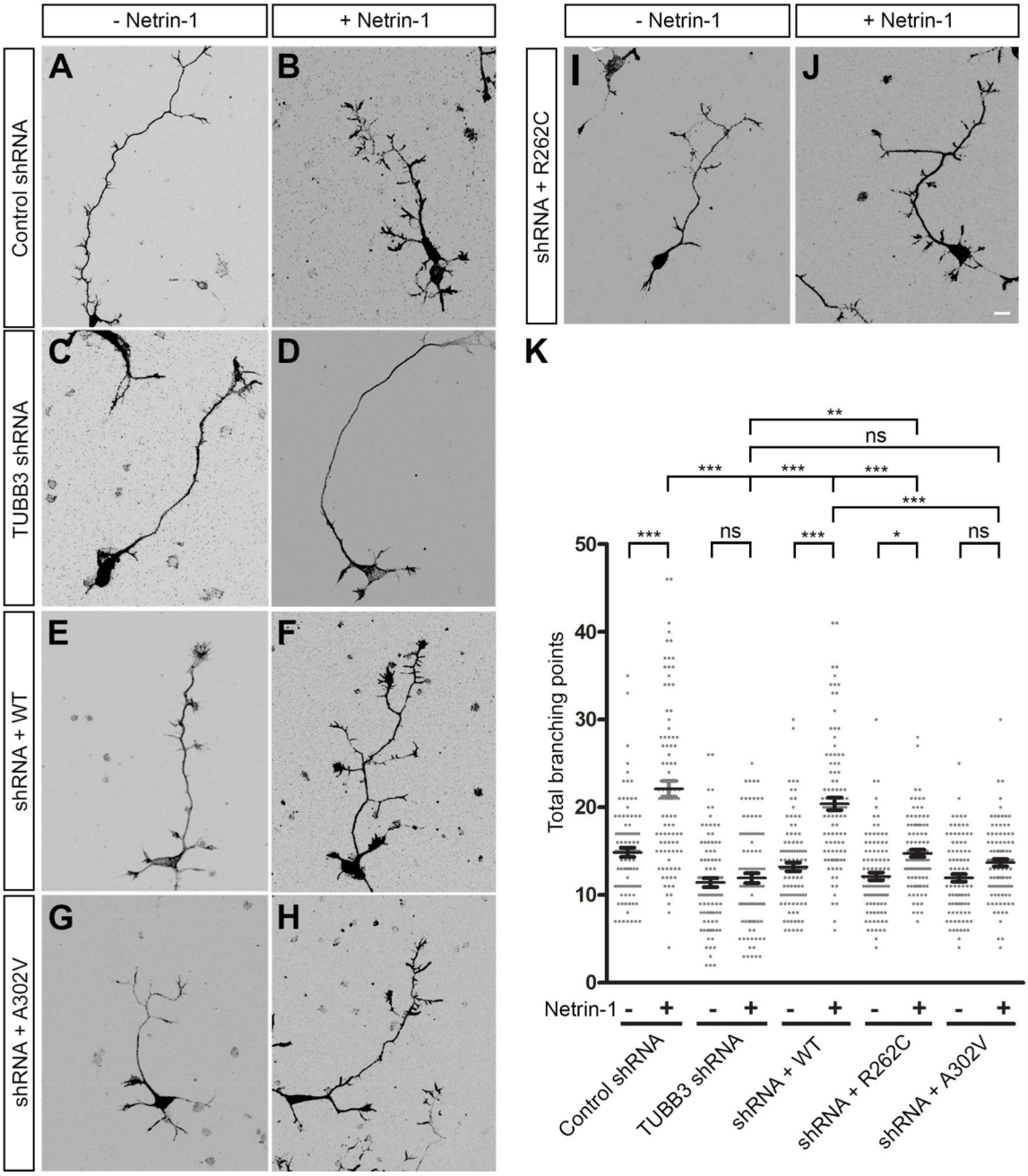

Figure 7.

TUBB3 mutations block netrin-1-induced axon branching of cortical neurons. A-J. Venus YFP was co-transfected with control shRNA (A, B), TUBB3 shRNAs (C, D), TUBB3 shRNAs plus wild type TUBB3 (E, F), TUBB3 shRNAs plus A302V (G, H) or TUBB3 shRNAs plus R262C (I, J) into E15 mouse cortical neurons. Primary neurons after nucleofection were cultured with purified netrin-1 (B, D, F, H and J) or sham-purified control (A, C, E, G, I) for 72 h. Scale bar: 10 μm. (K) Quantification of total branching numbers. 100 neurons/group from three independent experiments were analyzed. Data are

mean ± s.e.m. *p<0.05, **p<0.01, ***p<0.0001, ns indicates no significant difference (one-way Anova and Tukey's test for post-hoc comparisons).

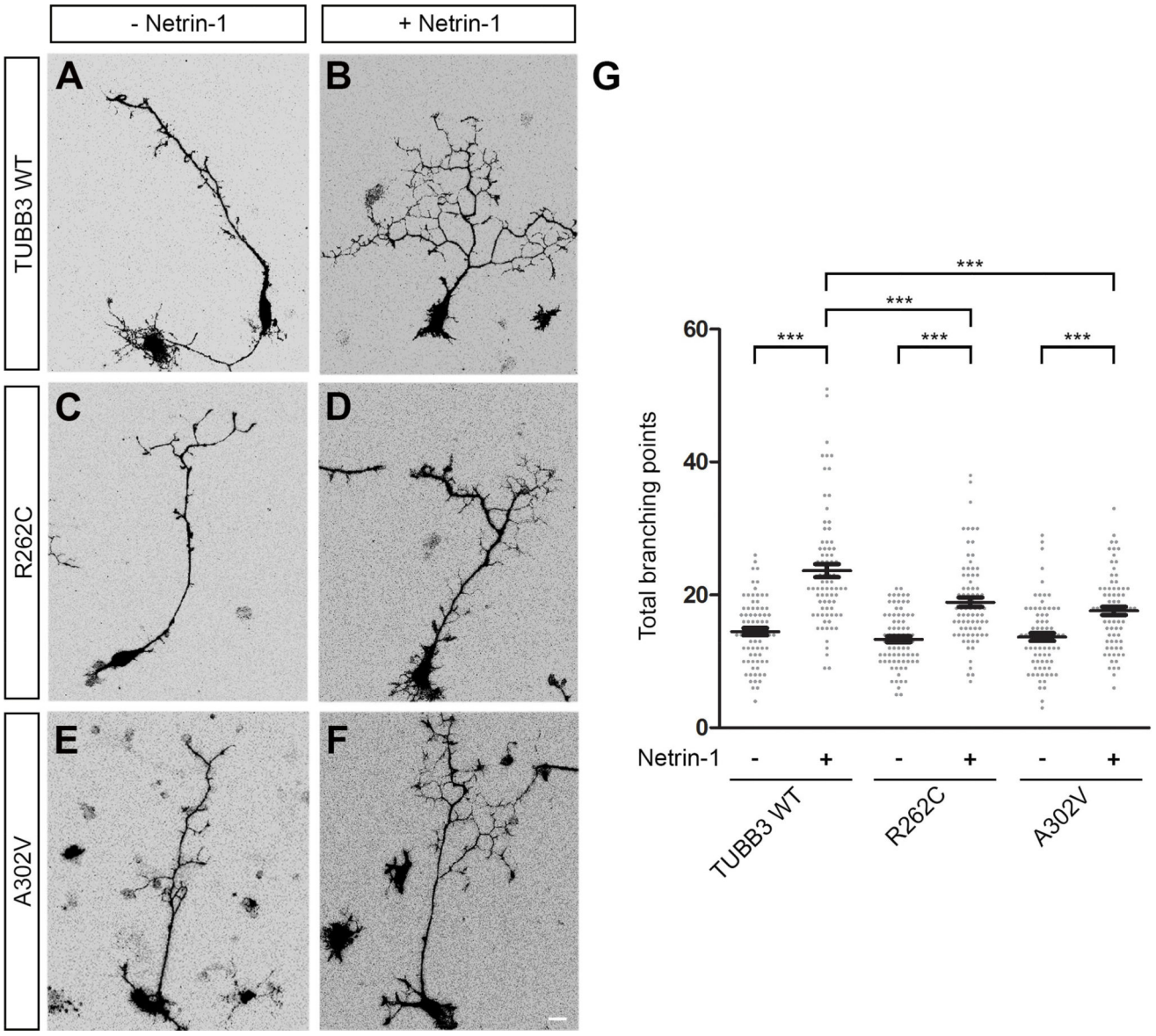

Figure 8.

Expression of either R262C or A302V in primary cortical neurons without knockdown of endogenous TUBB3 inhibits netrin-1-induced axon branching. A–F. Venus YFP was co-transfected with wild type TUBB3 (A, B), R262C (C, D), or A302V (E, F), into E15 mouse cortical neurons. Transfected neurons were incubated with purified netrin-1 (B, D, and F) or sham-purified control (A, C, and E) for 72 h. Scale bar: 10 μm. (G) Quantification of total branching numbers. 78 neurons/group from three independent experiments were analyzed. Data are mean ± s.e.m. ***$p<0.0001$ (one-way Anova and Tukey's test for post-hoc comparisons).

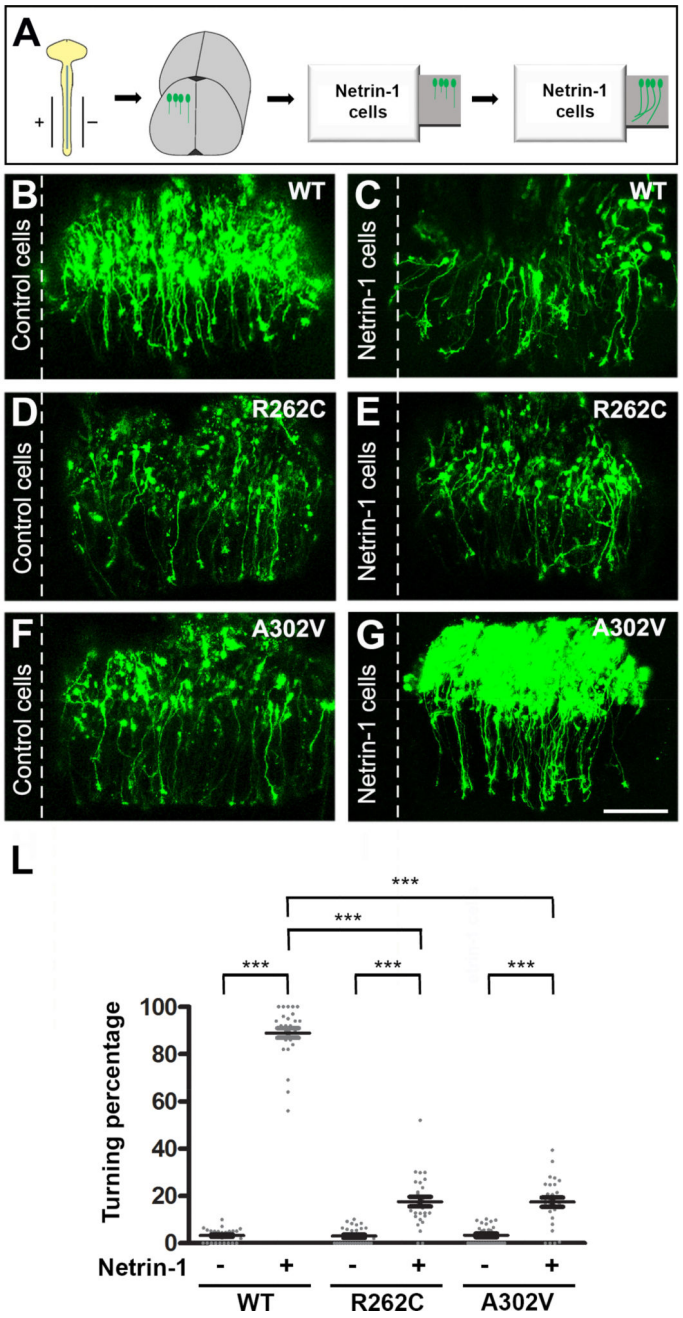

Figure 9.

TUBB3 mutations inhibit netrin-1-induced CA attraction. A. Schematic diagram showing *in ovo* electroporation and an open-book CA turning assay (Huang et al., 2015; Li et al., 2008; Liu et al., 2004; Liu et al., 2007; Liu et al., 2009; Qu et al., 2013a; Qu et al., 2013b). B–G. Venus YFP together with wild type human TUBB3 (B–C), R262C (D–E) or A302V (F–G) were electroporated into chick neural tubes and explants cultured with either netrin-1 cells (C, E and G) or control HEK293 cells (B, D and F). The scale bar is 100 μm. L. Quantification of axon turning. Data are mean ± s.e.m ***p<0.001 (One-way ANOVA with

Tukey's test for post-hoc comparisons). The axons from commissural neurons transfected with wild type TUBB3, but not R262C or A302V, were attracted to the netrin-1 source.

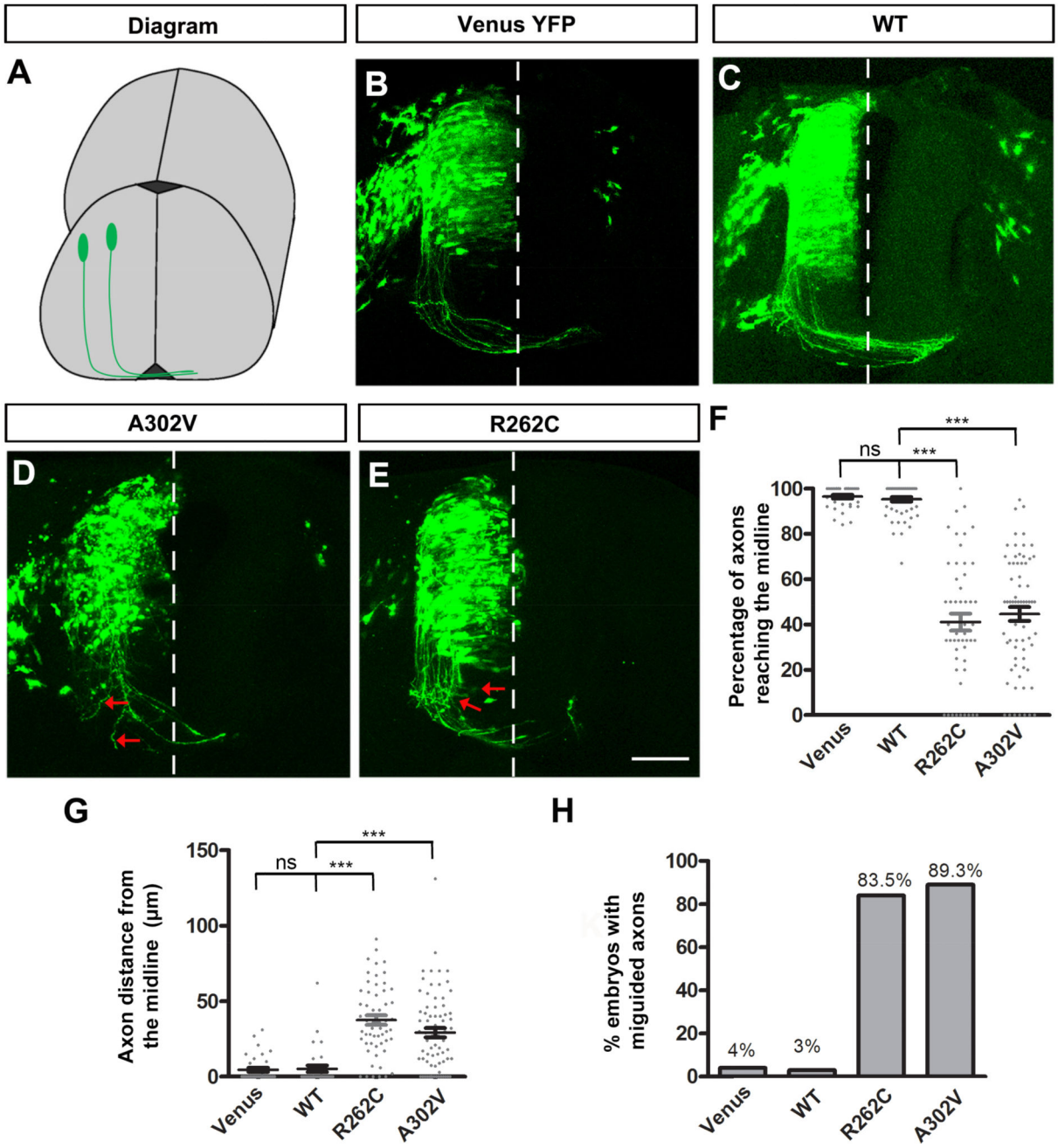

Figure 10. ***TUBB3*** **mutations disrupt spinal cord CA projection and pathfinding** ***in vivo***

A. Schematic diagram showing chick spinal cord CA projection after electroporation. B. The chick neural tube was electroporated with Venus YFP only. C. Chick commissural neurons were electroporated with Venus YFP plus wild type human TUBB3. D. Venus YFP plus A302V were electroporated into the chick neural tube. E. Commissural neurons with Venus YFP plus R262C. The red arrows in D and E point to misguided axons. Scale bar, 100 μm. F. Quantification of the percentage of axons reaching the midline. G. Quantification of the average distance of chick CAs away from the midline. H. The percentage of embryos with misguided axons. Data are presented as the mean ± s.e.m in F–G. ***p<0.001 (One-way

ANOVA with Tukey's test for post-hoc comparisons); ns, not significant. The numbers of embryos tested were: 12 (the Venus YFP group); 15 (the wild type human TUBB3 group; 14 (the A302V group); 14 (the R262C group).